NASA
Contractor Report 179611

AVSCOM
Technical Report 87-C-13

Computer Aided Design and Analysis of Gear Tooth Geometry

S.H. Chang and R.L. Huston
University of Cincinnati
Cincinnati, Ohio

May 1987

Prepared for the
Lewis Research Center
Under Grant NSG-3188

National Aeronautics and
Space Administration

TABLE OF CONTENTS

	Page Number
Chapter 1: Introduction	1
Chapter 2: One Parameter Enveloping and Gear Tooth Profile Generation	2
2.1 Introduction	3
2.2 Envelope of a Family of Curves	7
2.3 Development of Involute Spur Gear Teeth	10
2.4 Circular Arc As A Basic Rack	19
2.5 Tooth Profile Generated by a Straight Cutter on the Wheel	22
2.6 Reciprocal Conjugate Gear Tooth and Cutter Profile	29
Chapter 3: Bevel Gear Tooth Surface Generation	32
3.1 Introduction	32
3.2 Basic Theory	34
3.3 Bevel Gear Manufacturing	39
3.3.1 Bevel Gear Generation and Nongeneration	39
3.3.2 The Generating Process	41
3.3.3 The Basic Generator	42
3.3.4 Spiral Bevel Gear Cutting	43
3.4 Straight Bevel Gear Tooth Surface Generation	47
3.4.1 The Crown Rack	52
3.4.2 Straight Bevel Tooth Surface Equation	54
3.5 Spiral Bevel Gear Tooth Surface Generation	56
3.5.1 Kinematics Relation on the Machine Setting	56
3.5.2 Circular Cutter Surface	65
3.5.3 Spiral Bevel Gear Tooth Surface Equation	68
Chapter 4: Conclusion and Applications	73
Appendix A1. The Envelope of a Family of Curves	75
Appendix A2. Developable Surfaces	76
References	77

Chapter 1

Introduction

Over the past fifteen years, interest has continued to grow in the study of gearing technology. There have been increasing demands for improved power transmission. The major areas for improving transmission systems are in higher power-to-weight ratios, better control of transmission vibration, reduced noise, increased reliability, and longer life. To obtain these improvements, it is necessary to have a thorough understanding of the stresses, the dynamic loading, the contact forces, the vibration and the noise characteristics, the lubrication phenomena and the fatigue life. For example, gear lubrication technology involves the Hertz contact stress, the elastohydrodynamic film thickness, and the flash temperature. These are the major factors in tooth surface scuffing. The understanding of these phenomena requires a knowledge of the relative curvature of the contacting tooth profiles and of their relative velocities. This is a problem of the tooth geometry. This problem is addressed in this report.

Specifically, the report is concerned with a computer analysis of the geometry of gears. It presents a new modeling method to simulate the gear manufacturing machining processes, such as gear hobbing, and straight and spiral bevel gear machining. The method is based on the work in reference [1]*, allowing for both standard and nonstandard gear tooth modelling.

---

*Numbers appearing in square brackets refer to references at the end of the report.

Further, it discusses the procedures for the cutter design. The kinematic relations for the tooth surfaces of spur and bevel gears are presented. The results and procedures are expected to form a basis for improved gear design.

The balance of the report is divided into three chapters. In the following chapter a model of the gear hobbing process is presented. A gear tooth profile generation theory is also derived. The development of the nonstandard tooth profiles, and the development of reciprocal conjugate gear tooth cutter is discussed. In the next chapter the procedures are generalized to three-dimensions. The basic theory of the bevel gear and its manufacturing method are briefly discussed. The machining mechanisms for straight and spiral bevel gears are modeled. The tooth surface equations of the straight and spiral bevel gear are derived in curvilinear parametric form. The final chapter presents a summary of the methods. It discusses applications and suggestions for the future research.

Chapter 2

One Parameter Enveloping and Gear Tooth Profile Generation

2.1 Introduction

Recent advances in computer graphics and computer aided design present an opportunity for developing new procedures for optimizing gear tooth geometry. In this chapter, a procedure for generating tooth profiles is presented. It employs the envelope of a one-parameter family curves. The focus is upon 2-dimension standard and nonstandard gear teeth, but the same approach may be applied with 3-dimension gear teeth, such as with straight, and spiral bevel gears.

The basic concepts underlying the method are readily seen by considering the hob cutter process for fabricating spur gear teeth. This process is based upon the concept of a reciprocating rack cutter with straight teeth moving across a gear blank as depicted in Figure 2.1.1. Geometrically this process may be viewed as a series of inclined line segments intersecting the circular gear blank, with the envelope of the line segments forming the tooth profile as shown in Figure 2.1.2 [2].

A second way of viewing this process is to imagine a perfectly plastic wheel rolling over a "step" or obstacle in the form of a rack tooth as shown in Figure 2.1.3. The impression (or "footprint") forms the gear tooth profile. It is well known that this tooth profile is an involute of a circle. That is, the envelope of the line segments on the gear blank is an involute of a circle.

Recall that the involute of a circle may be viewed as the locus of the end of a cord being unwrapped around a circle. If the circle has infinite

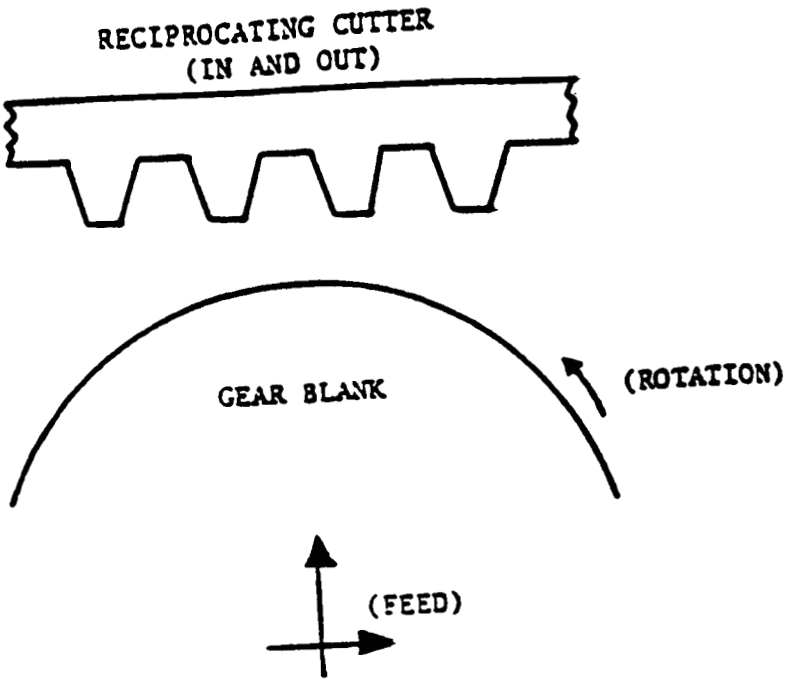

Figure 2.1.1. Reciprocating Rack Cutter and Gear Blank

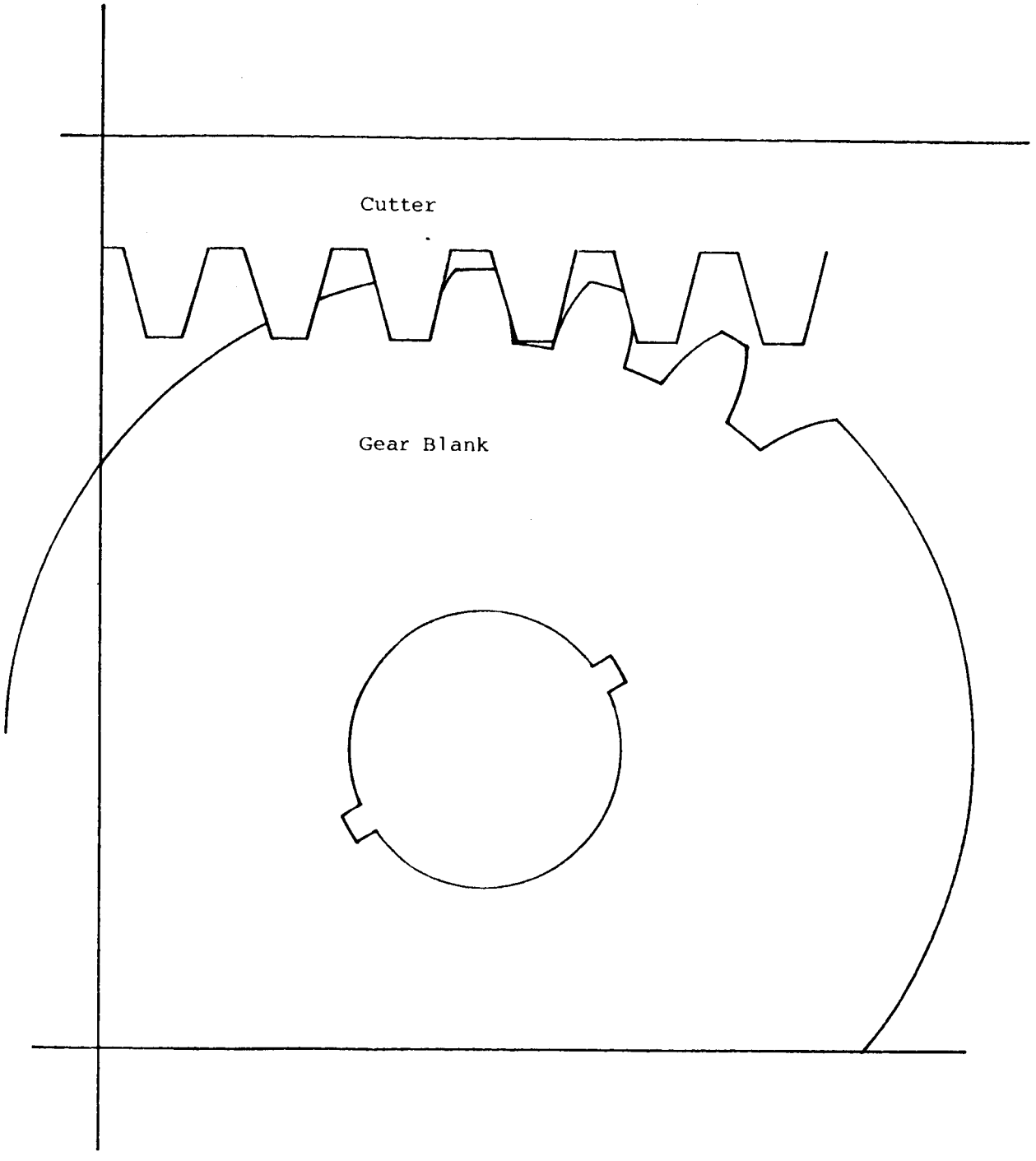

Figure 2.1.2 Generation of an Involute Tooth Profile By a Rack Cutter

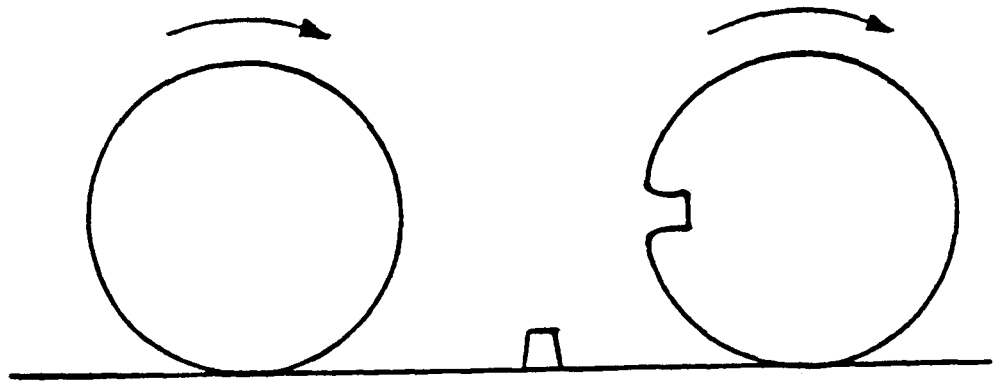

Figure 2.1.3. Wheel Rolling Over a Rack Tooth Forming the Tooth Profile

radius, the involute will be straight, as with the rack tooth.

2.2 Envelope of a Family of Curves

Consider a plane curve C as shown in Figure 2.2.1. Analytically C may be represented by an equation of the form $y = f(x)$. Suppose in this functional description we introduce a parameter t defining a family of similar curves. Suppose further that as t changes the orientation of the curves change and that they intersect each other as in the figure. The curve E, tangent to the intersection curves is then the envelope of the family [3].

It is relatively easy to obtain an analytical expression for the envelope. To see this, let the representation of the family of curves be $y = f(x, t)$ or $F(x, y, t) = 0$ where t is the motion parameter. If t is replaced by $t + \Delta t$ where Δt is a small increment in t, the expression $F(x, y, t + \Delta t) = 0$ also represents a member of the family of curves. Hence, the "difference quotient" $[F(x, y, t + \Delta t) - F(x, y, t)]/\Delta t = 0$ is a member of the family as well. Therefore, by a limiting process, a second expression for members of the family of the curves is $\partial F(x, y, t)/\partial t = 0$. By eliminating t between F and $\partial F/\partial t$ we obtain an equation of the form $G(x, y) = 0$. $G(x, y)$ thus represents the locus of points common to $F = 0$ and $\partial F/\partial t = 0$. That is, $G(x, y)$ represents the points on the envelope E and is thus the desired analytical representation of E. (See Appendix A for additional details.)

To illustrate these ideas, consider the envelope of a family of lines, each a distance r from a fixed point O as depicted in Figure 2.2.2. Let ϕ

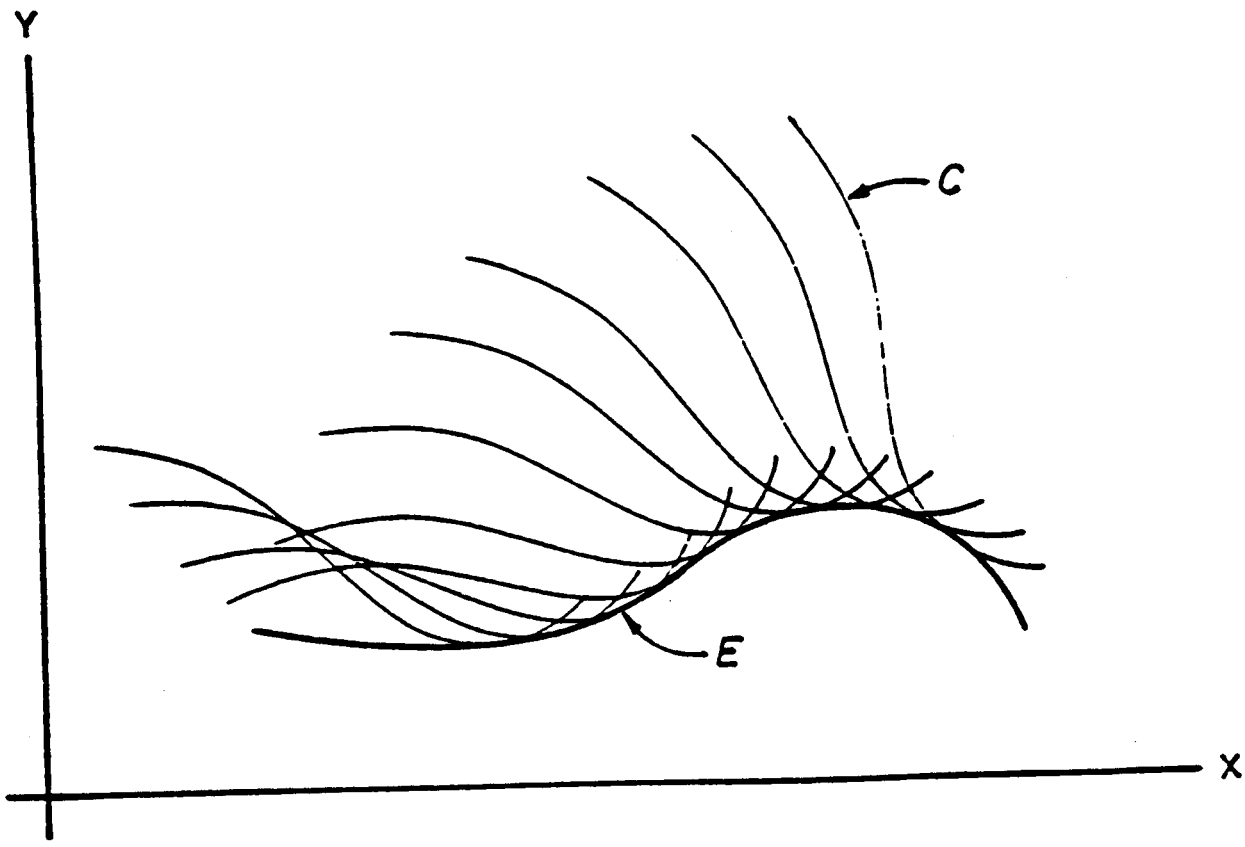

Figure 2.2.1. A Family of Intersecting Curve

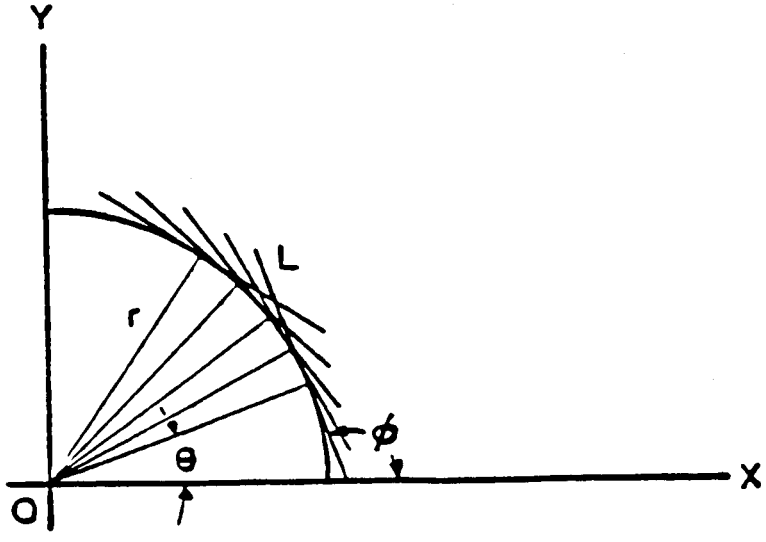

Figure 2.2.2. A Family of Line Equidistant from a Point

be the inclination angle of a typical member L of the family and let ϕ be the inclination angle of a typical member L of the family and let θ be the inclination of the line normal to L and passing through O as shown. The equation of L might be written as:

$$y - y_p = m(x - x_p) \tag{2.2.1}$$

where m is the slope of L and (x_p, y_p) are the coordinates of P, the point of intersection of L and its normal line through O. But, $m = \tan\phi$ and $\tan\phi = -\cos\theta$. Also x_p and y_p may be expressed as $r\cos\theta$ and $r\sin\theta$. Hence, the equation of L might be rewritten as:

$$y - r\sin\theta = (-\cot\theta)(x - r\cos\theta) \tag{2.2.2}$$

or as:

$$y\sin\theta + x\cos\theta - r = 0 = F(x, y, \theta) \tag{2.2.3}$$

Equation (2.2.3) may be considered as defining the family of the lines with θ being the family parameter. By differentiating with respect to θ, we have

$$\frac{\partial F}{\partial \theta} = y\cos\theta - x\sin\theta = 0 \tag{2.2.4}$$

Finally, the equation of the envelope may be obtained by solving equations (2.2.3) and (2.2.4) for x and y, leading to the expression:

$$x = r\cos\theta \quad \text{and} \quad y = r\sin\theta \tag{2.2.5}$$

or by eliminating θ as:

$$x^2 + y^2 = r^2 \tag{2.2.6}$$

The envelope, as expected, is a circle, with the family of lines being tangent to the circle.

2.3 Development of Involute Spur Gear Teeth

A similar procedure can be used to examine a spur gear tooth profile. Consider again Figure 2.1.3 where the involute profile is generated by the step's impression on the plastic wheel. To describe the impression we need to find the envelope, in the wheel, of the line segments representing the sides of the step. To this end, consider Figure 2.3.1 where L is a step side, line segment. L is inclined at an angle ϕ to the X-axis and it intersects the X axis at a distance x_0 from the origin. The wheel W has a radius r, center $\hat{O}$, and roll angle θ. $\hat{X}$ and $\hat{Y}$ are coordinate axes fixed in W with origin at $\hat{O}$. The objective is then to express the envelope of L in the $\hat{X}$-$\hat{Y}$ system.

Let (x, y) and ($\dot{x}$, $\dot{y}$) be coordinates of a typical point P on L, relative to the X-Y and $\hat{X}$-$\hat{Y}$ systems. Then it is shown that x and y are related with $\hat{x}$ and $\hat{y}$ by the expression:

$$x = r\theta + \hat{x}\cos\theta + \hat{y}\sin\theta \tag{2.3.1}$$

and

$$y = r - \hat{x}\sin\theta + \hat{y}\cos\theta \tag{2.3.2}$$

The equation of L is

$$y = (x - x_0)\tan\phi \tag{2.3.3}$$

Using equations (2.3.1) and (2.3.2), L may be described in terms of $\hat{x}$ and $\hat{y}$ as:

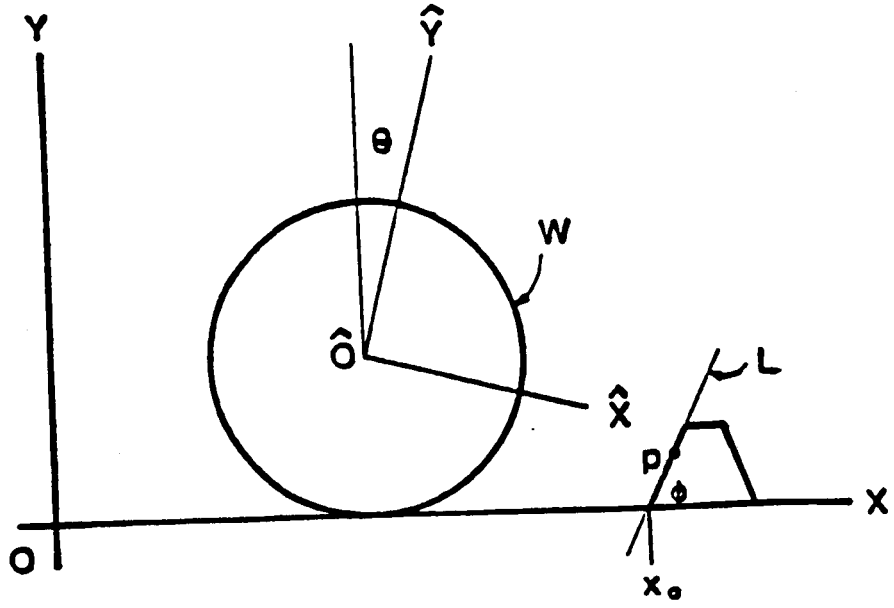

Figure 2.3.1. Representation of a Perfect Plastic Wheel Rolling Over a Step

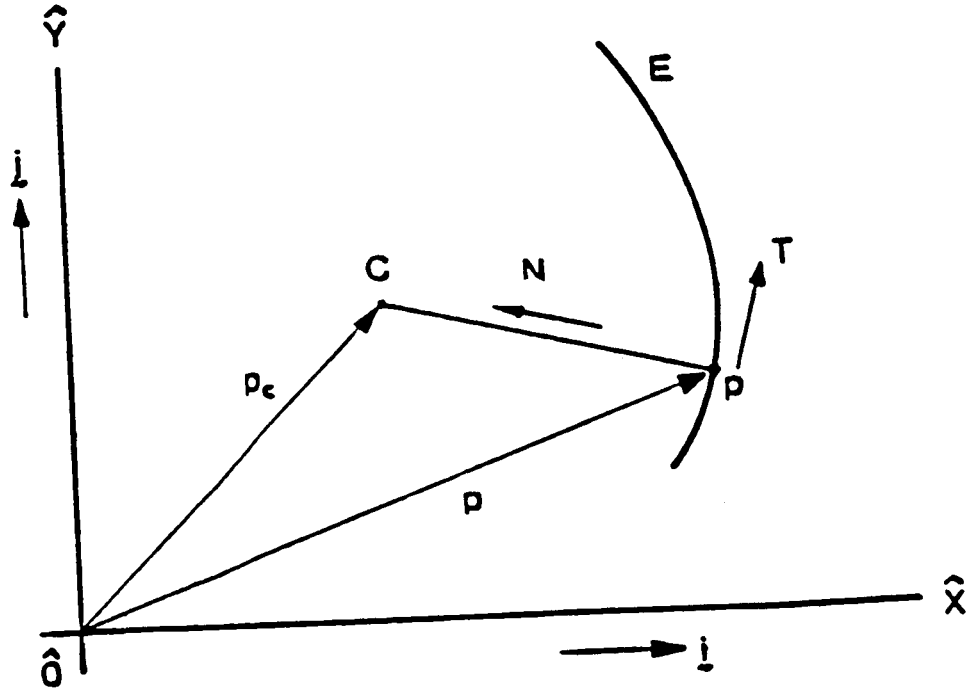

Figure 2.3.2. The Center of Curvature C at a Typical Point P of the Envelope

$$\hat{y}(\cos\theta - \tan\phi \sin\theta) - \hat{x}(\sin\theta + \tan\phi \cos\theta)$$

$$+ r + (x_0 - r\theta)\tan\phi = 0 = F(\hat{x}, \hat{y}, \theta) \qquad (2.3.4)$$

Equation (2.3.4), like equation (2.2.3) can be considered as describing a family of lines relative to X-Y system with θ being the parameter. Hence, by differentiating equation (2.3.4) with respect to θ, we have:

$$\frac{\partial F}{\partial \theta} = 0 = \hat{y}(\sin\theta + \tan\phi \cos\theta)$$

$$+ \hat{x}(\cos\theta - \tan\phi \sin\theta) + r\tan\phi \qquad (2.3.5)$$

By solving equations (2.3.4) and (2.3.5) for $\hat{x}$ and $\hat{y}$, we obtain:

$$\hat{x} = r\sin\theta + (x_0 - r\theta)\sin\phi \cos\phi(\sin\theta + \tan\phi \cos\theta)$$

$$\hat{y} = -r\cos\theta - (x_0 - r\theta)\sin\phi \cos\phi(\cos\theta - \tan\phi \sin\theta) \qquad (2.3.6)$$

Equations (2.3.6) are a pair of parametric equations representing the envelope of L relative to W. Therefore, equations (2.3.6) describe the tooth profile impression created by the cutter step.

Let P be a typical point of the envelope E (See Figure 2.3.2.). The radius of curvature ρ of E at P may be expressed as [4, 5].

$$\rho = \frac{(\hat{x}_\theta^2 + \hat{y}_\theta^2)^{3/2}}{\hat{y}_{\theta\theta}\hat{x}_\theta - \hat{x}_{\theta\theta}\hat{y}_\theta} \qquad (2.3.7)$$

where the subscript θ indicates partial differentiation with respect to θ. By substituting from equations (2.3.6) into (2.3.7), ρ takes the relatively simple form:

$$\rho = \frac{1}{[r\cos\phi + (x_0 - r\theta)\sin\phi]} \qquad (2.3.8)$$

The center of curvature C of E at P is located on a line perpendicular to E at a distance ρ from E. Hence, C may be located relative to the wheel center $\hat{O}$ by the vector $\underset{\sim}{p} + \rho\underset{\sim}{N}$, where $\underset{\sim}{p}$ locates P relative to O and $\underset{\sim}{N}$ is a unit vector perpendicular to E as shown in Figure 3.3.2. Recall that a unit vector $\underset{\sim}{T}$ tangent to E at P may be expressed as [5]:

$$\underset{\sim}{T} = \frac{(\hat{x}_\theta \underset{\sim}{i} + \hat{y}_\theta \underset{\sim}{j})}{(\hat{x}_\theta^2 + \hat{y}_\theta^2)^{\frac{1}{2}}} \tag{2.3.9}$$

Hence, $\underset{\sim}{N}$ may be written as:

$$\underset{\sim}{N} = (-\hat{y}_0 \underset{\sim}{i} + \hat{x}_0 \underset{\sim}{j})/\hat{x}_0^2 + \hat{y}_0^2)^{\frac{1}{2}} \tag{2.3.10}$$

Let $\underset{\sim}{p}_C$ be the vector from $\hat{O}$ to C. Then, using equation (2.3.7), $\underset{\sim}{p}_C$ may be written as:

$$\underset{\sim}{p}_C = \underset{\sim}{p} + p\underset{\sim}{N} = \hat{x}_C\underset{\sim}{i} + \hat{y}_C\underset{\sim}{j}$$

$$= \hat{x}\underset{\sim}{i} + \hat{y}\underset{\sim}{j} + (-\hat{y}_0\underset{\sim}{i} + \hat{x}_0\underset{\sim}{j})(\hat{x}_0^2 + \hat{y}_\theta^2)/(\hat{x}_0\hat{y}_{00} - \hat{y}_0\hat{x}_{00}) \tag{2.3.11}$$

where (x_C, y_C) are the coordinates of C relative to the X-Y system, fixed in W. By substituting from equations (2.3.6) and by performing the indicated differentiations, it is seen that the ratio $(\hat{x}_0 + \hat{y}_0)/(\hat{x}_0\hat{y}_{00} - \hat{y}_0\hat{x}_{0\theta})$ is unity and that $\hat{x}_C$ and $\hat{y}_C$ are:

$$\hat{x}_C = \hat{x} - \frac{\partial\hat{y}}{\partial\theta} = -r(\cos\theta - \tan\phi\,\sin\theta)\sin\phi\,\cos\phi$$

and

$$\hat{y}_C = \hat{y} + \frac{\partial\hat{x}}{\partial\theta} = -r(\sin\theta + \tan\phi\,\cos\theta)\sin\phi\,\cos\phi \tag{2.3.12}$$

The locus of the centers of curvature can be seen to be a circle. That is, from equations (3.3.12), we find that

$$\hat{x}_c^2 + \hat{y}_c^2 = r^2 \sin^2\phi \qquad (2.3.13)$$

By recalling the construction of an involute as the locus of the end points of an unwrapping cord around a circle, we see that the cord is perpendicular to the involute and its unwrapped length is the radius of curvature of the involute. Hence, the centers of curvature of the envelope are located on the generating circle, also called the "evolute." Therefore, the envelope E of the step of Figure 2.3.1 is the involute of the circle of equation (2.3.6).

Recall that for a spur gear the circle generating the involute tooth profile is called the base circle. Recall also that if meshing spur gears are viewed as rolling cylinders, the cylinder cross sections define the pitch circles. Then, if the pressure angle is defined as the angle between the radial line and the tooth profile at the pitch circle, it is readily seen [6] that the ratio of the radii of the base and pitch circle is

$$\frac{R_B}{R_P} = \cos\psi \qquad (2.3.14)$$

In the above analysis, the wheel profile is the pitch circle, the pressure angle is the compliment of ϕ, (that is, $\cos\psi = \sin\phi$), and the generating circle is the locus of the centers of curvature of the involute (the evolute). Then, from equation (2.3.13), the base circle radius if $r\sin\phi(=r\cos\psi)$ where r is the pitch circle radius. Therefore, the ratio of the radii of the base and pitch circles is simply $\sin\phi$, or $\cos\psi$--a result consistent with equation (2.3.14).

To demonstrate these results, the line segments generating the envelope were plotted for $r = 1$, $\phi = 70°$, $x_o = 0.70021$, and $0 \leq \theta \leq 720$.

Figure 2.3.3 shows the results for 9.6 deg. increments in θ. Figure 2.3.4 shows a computer drawn graph of equation (2.3.6). The "natural" envelope in Figure 2.3.3 is thus seen to be the same as the "analytical" envelope of Figure 2.3.4. Figure 2.3.5 shows a computer generated drawing of the base circle, the pitch circle, and an involute curve forming a portion of a tooth profile.

These results may be summarized as follows:

1. The envelope of an inclined line on a rolling wheel is an involute.
2. The evolute of an envelope is a circle.
3. The rolling wheel is the pitch circle of a spur gear.
4. The evolute is the base circle.
5. Inclination angle is the pressure angle.

A major application of this procedure is with the computer aided design and analysis of nonstandard tooth profiles. For example, suppose that the cutter profile is not straight, but instead has a profile defined by the expression $y = f(x)$ (instead of $y = (x - x_0)\tan\phi$ as equation (2.3.3)). Then, in terms of the X-Y coordinate system of the gear blank, the resulting tooth profile is determined from the expressions:

$$r - x\sin\theta + y\cos\theta - f = 0 \qquad (2.3.15)$$

and

$$-x\cos\theta - y\sin\theta - (r - x\sin\theta + y\cos\theta)f' = 0 \qquad (2.3.16)$$

where from equation (2.3.5) the argument of f is $(r + x\cos\theta + y\sin\theta)$ and where f' is the derivative of f with respect to its argument. When equations (2.3.15) and (2.3.16) are solved for x and y in terms of θ, they

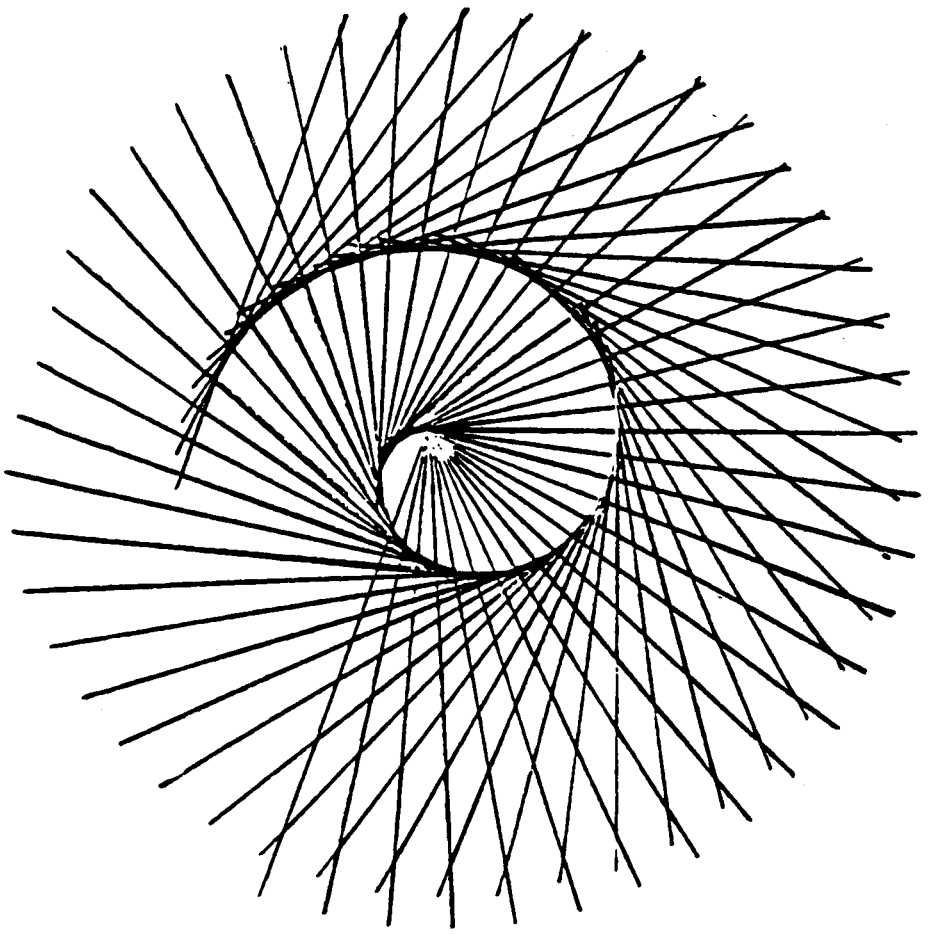

Figure 2.3.3. Computer Drawn Cutting Lines at 9.6° Intervals for $\phi = 70$, $r = 1$, $x_0 = 0.70021$, and $0 \leq \theta \leq 720$.

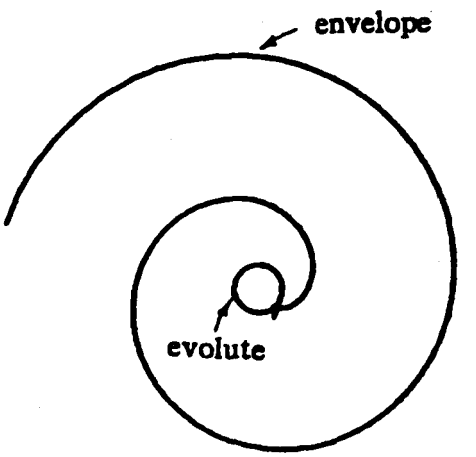

Figure 2.3.4. Graph of Equation 3.3.6.

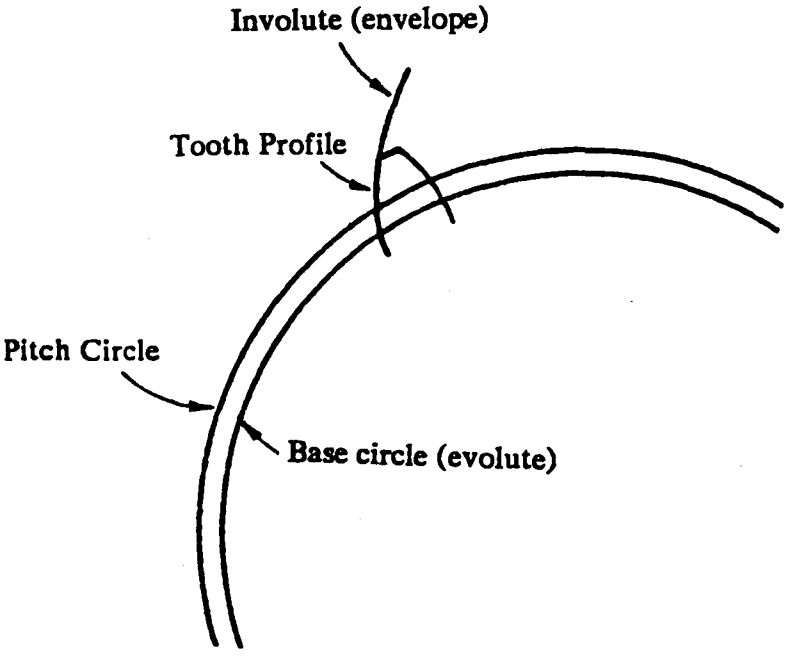

Figure 2.3.5. Computer Drawing of Base Circle, Pitch Circle, and Involute

form a pair of parametric equations for the envelope of the cutter profile, which is the tooth profile. The following section contains an example of a nonstandard tooth profile generated by this procedure.

A second major application of the procedure is with the design and analysis of bevel, spiral bevel, and hypoid gears. In this case, the procedures are generalized to three dimensions, and the cutter surface creates a family of surfaces whose envelope in the gear blank is the tooth surface. When these procedures are developed numerically, the resulting representation of the tooth surface appears in a form suitable for kinematic, stress, and life analysis. In Chapter 3 these ideas are discussed by examining the envelope of a conical cutter surface onto a mating rolling cone.

2.4 Circular Arc As A Basic Rack

As noted in Section 2.3, a non-straight basic-rack profile can be used to form a nonstandard gear tooth profile. This is demonstrated in Figure 2.4.1 where an arc of a circle is used as a cutter. In the figure, the coordiante axes X and Y are fixed, B is the distance along the X axis, and D is the distance along the Y axis to the circle center. The plastic wheel W has a radius r, center $\hat{O}$, and roll angle θ. $\hat{X}$ and $\hat{Y}$ are coordinate axes fixed in W. The initial position of W is at a distance x_0 from the origin of X-Y coordinates.

Let (x, y) and ($\hat{x}$, $\hat{y}$) be coordinates of a typical point P on C, relative to the X-Y and $\hat{X}$-$\hat{Y}$ systems. Then it is seen that $\hat{x}$ and $\hat{y}$ are related to x and y by the expressions:

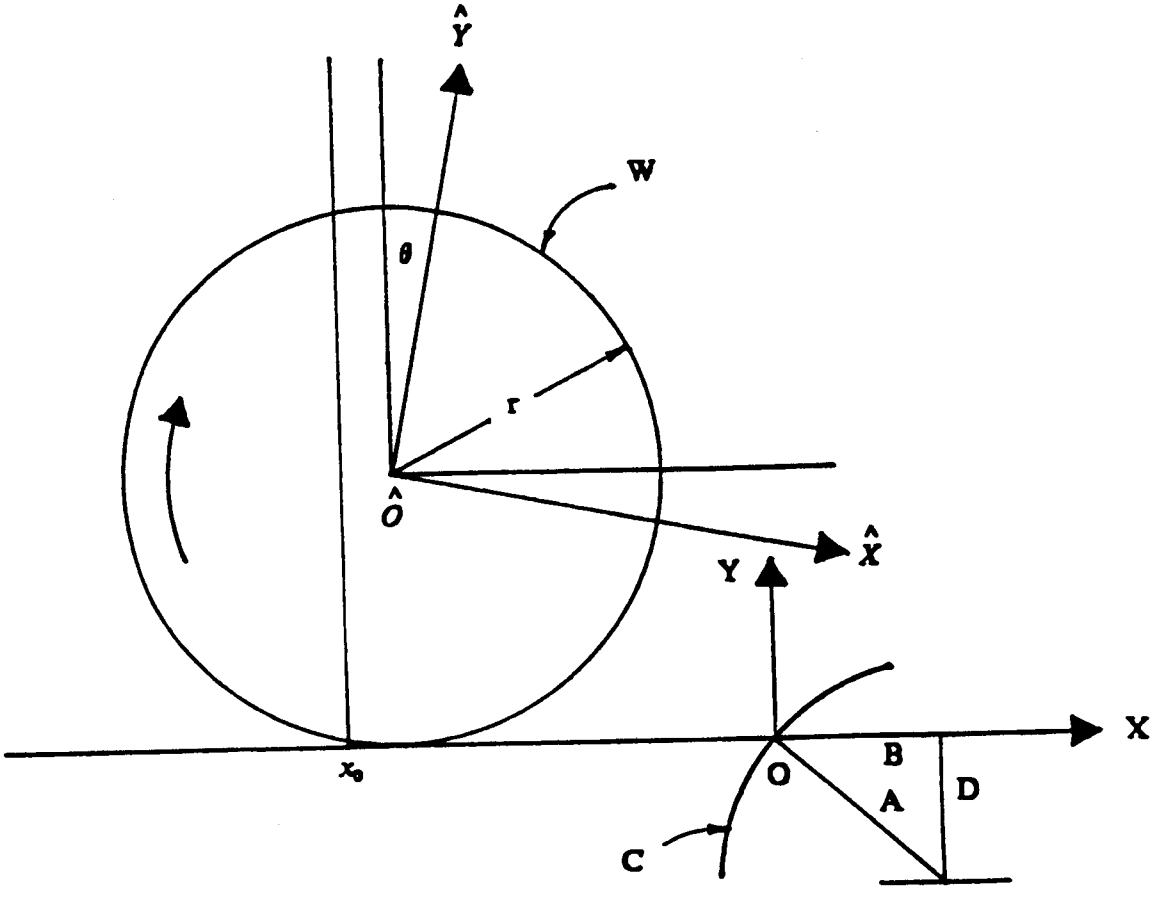

Figure 2.4.1. Circular Arc as a Basic Rack

$$x = (r\theta - x_0) + \hat{x}\cos\theta + \hat{y}\sin$$

and

$$y = r - \hat{x}\sin\theta + \hat{y}\cos\theta \tag{2.4.1}$$

A point P (x, y) on the arc C may be located from the expession:

$$x = B - \sqrt{A^2 - (D + y)^2} \tag{2.4.2}$$

where A is the radius of the circle.

By differentiating equation (2.4.2) with respect to y, we obtain:

$$\frac{dx}{dy} = \tan\phi = \frac{(D + y)}{\sqrt{A^2 - (D + y)^2}} \tag{2.4.3}$$

Using equations (2.4.2) and (2.4.3), C may be expressed in terms of $\hat{x}$ and $\hat{y}$ as:

$$(r\theta - x_0 - B) + \hat{x}\cos\theta + \hat{y}\sin\theta + \sqrt{A^2 - (D + r - \hat{x}\sin\theta + \hat{y}\cos\theta)^2} = 0 = F(\hat{x}, \hat{y}, \theta) \tag{2.4.4}$$

Equation (2.3.4), like equation (3.2.3) can be considered as describing a family of lines relatve to the X-Y system with θ being the parameter. Hence, by differentiating equation (2.4.4) with respect to θ, we have:

$$\frac{\partial F}{\partial \theta} = 0 = r - \hat{x}\sin\theta + \hat{y}\cos\theta + \frac{(D + r - x\sin\theta + y\cos\theta)(x\cos\theta + y\sin\theta)}{\sqrt{A^2 - (D + r - \hat{x}\sin\theta + \hat{y}\cos\theta)^2}} = 0 \tag{2.4.5}$$

Equations (2.4.4) and (2.4.5) form a simultaneous system of nonlinear equations representing the envelope of the cutter relative to the gear blank. The solution describes the tooth profile impression created by the cutter.

To illustrate the use of equation (3.4.5), the envelope of the circular step on the roller was plotted for x_0 = 7.131 in, A = 5. in, D = 2.1131 in, and r = 20. in. Figure 2.4.2 shows the results. The other curve shown in the figure was plotted using Buckingham's equation [7]. The other curve shown in the figure was plotted using Buckingham's equation [7]. The two curves are identical if they are superimposed. The circular arc shown in the figure represents the roller.

2.5 Tooth Profile Generated by a Straight Cutter on the Wheel

Another procedure for generating involute gears is to use a pinion-shaped cutter in a shaping or planing machine. Both the cutter and gear blank are revolved as gears between each stroke of the machine. This method is extensively used in the automotive industries for finishing gears which have been roughed out on a gear milling or hobbing machine [2]. This section describes the simulation of this shaping process.

Consider Figure 2.5.1. Let L be a line segment step side to simulate the cutter. L is inclined at an angle ϕ to the radial line OE, and point E on the wheel is located by an angle α. The wheel W has a radius R, center O, and is fixed. X and Y are coordinate axes fixed in W with origin at O. The roller G has a radius r, center $\hat{O}$, and roll angle $\hat{\theta}$. $\hat{X}$ and $\hat{Y}$ are coordinate axes fixed in G with origin at $\hat{O}$. The objective is then to express the envelope of L in the $\hat{X}$-$\hat{Y}$ system.

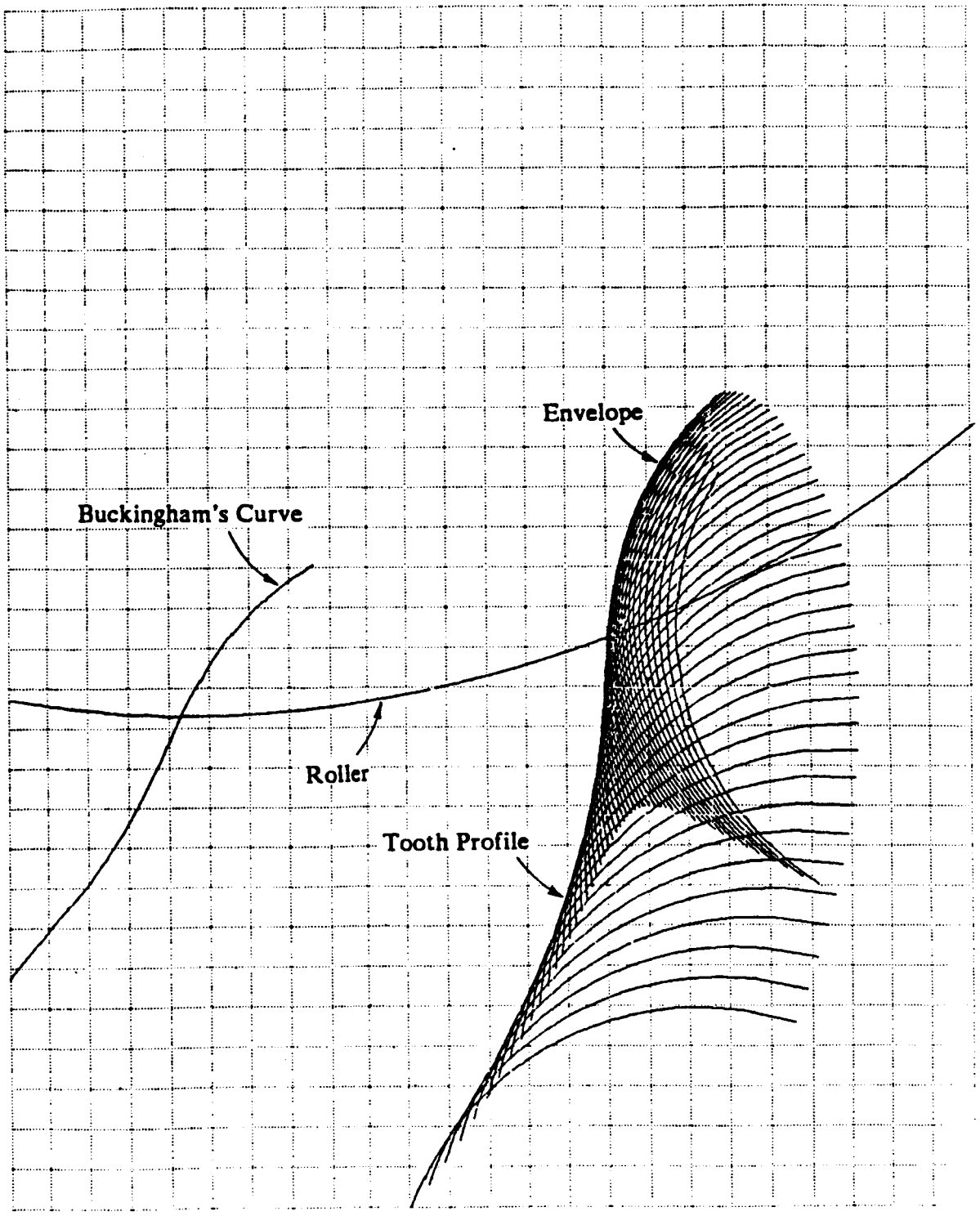

Figure 2.4.2. Nonstandard Gear Tooth Profile

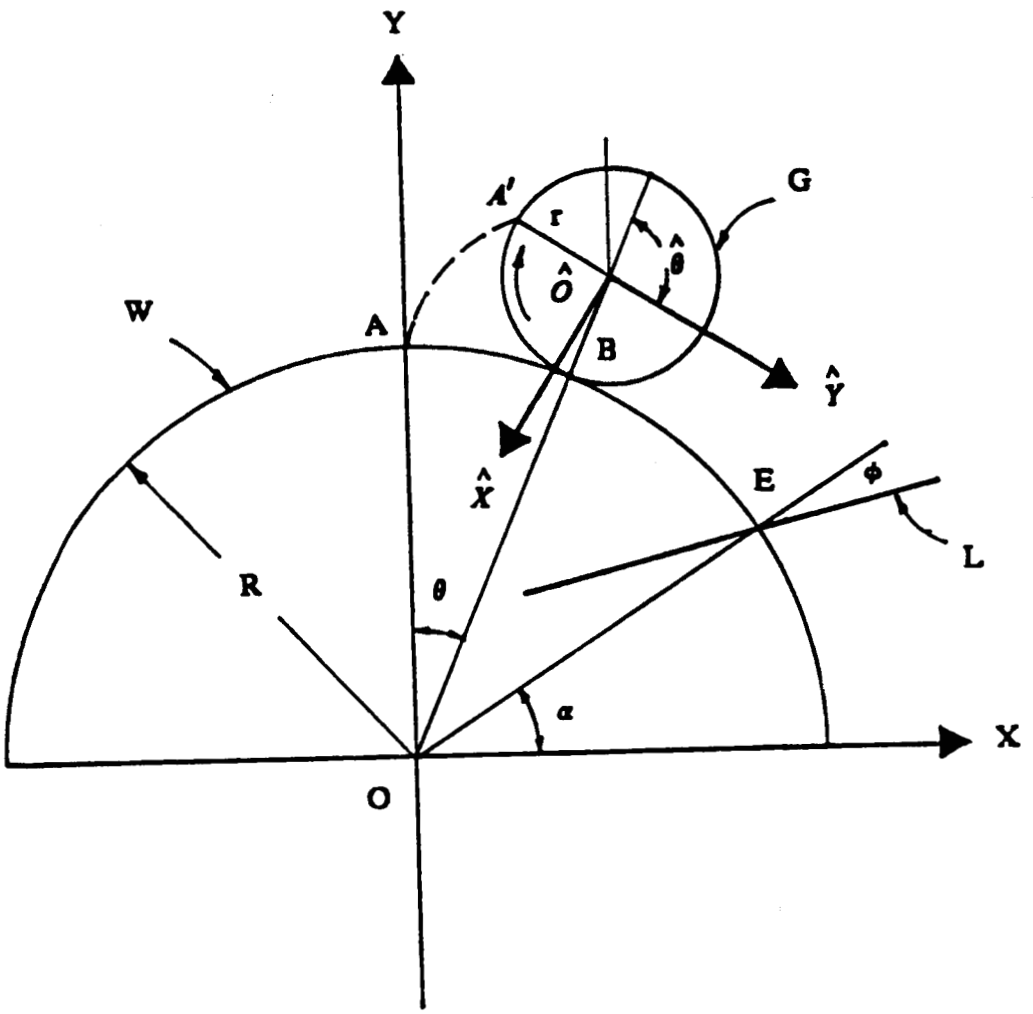

Figure 2.5.1. Roller Rolling Over a Straight Line on a Wheel

The roller rolls on the wheel without slipping. When the roller rolls from position A to position B, it rotates through the angle $\hat{\theta}$. Angle $\hat{\theta}$ and are then related by the expression:

$$R\theta = r\hat{\theta} \tag{2.5.1}$$

Let (x, y) and ($\hat{x}$, $\hat{y}$) be coordinates of a typical point P on L, relative to the X-Y and $\hat{X}$-$\hat{Y}$ systems. Then it is shown that $\hat{x}$ and $\hat{y}$ are related to x and y by the expressions:

$$x = (R + r)\sin\theta + \hat{x}\cos(0 + \hat{0}) + \hat{y}\sin(\theta + \hat{\theta})$$

and

$$y = (R + r)\cos 0 - \hat{x}\sin(\theta + \hat{\theta}) + \hat{y}\cos(\theta + \hat{\theta}) \tag{2.5.2}$$

The equation of L is:

$$\tan(\alpha - \phi)(x - R\cos\alpha) = (y - R\sin\alpha) \tag{2.5.3}$$

Where $\tan(\alpha - \phi)$ is the slope of L. $(R\cos\alpha, R\sin\alpha)$ are the coordinates of E, the point of intersection of L and the wheel.

Using equations (2.5.1) and (2.5.2), L may be expressed in terms of $\hat{x}$ and $\hat{y}$ as:

$$\begin{aligned}&\hat{x}[\tan(\alpha - \phi)\cos(0 + \hat{0}) + \sin(0 + \hat{0})]\\ &+ \hat{y}[\tan(\alpha - \phi)\sin(0 + \hat{0}) - \cos(0 + \hat{\theta})]\\ &+ \tan(\alpha - \phi)[(R + r)\sin(\theta) - R\cos\alpha]\\ &- (R + r)\cos(\theta) + R\sin\alpha = 0\end{aligned} \tag{2.5.4}$$

By substituting (2.5.1) into (2.5.4), we have:

$$\hat{x}[\tan(\alpha - \phi)\cos(\frac{r + R}{R})\hat{\theta} + \sin(\frac{r + R}{R})\hat{\theta}]$$

$$+ \hat{y}[\tan(\alpha - \phi)\sin(\frac{r + R}{R})\hat{\theta} - \cos(\frac{r + R}{R})\hat{\theta}]$$

$$+ \tan(\alpha - \phi)[(R + r)\sin(\frac{r}{R})\hat{\theta} - \cos\alpha]$$

$$- (R + r)\cos(\frac{r}{R})\hat{\theta} + R\sin\alpha = 0 = f(\hat{x}, \hat{y}, \hat{\theta}) \qquad (2.5.5)$$

Equation (2.5.5) may be considered as a one-parameter family lines and $\hat{\theta}$ is the parameter. By differentiating equation (2.5.50 with respect to $\hat{\theta}$. We have:

$$\frac{\partial f(\hat{x}, \hat{y}, \hat{\theta})}{\partial \hat{\theta}} =$$

$$- \hat{x}[\tan(\alpha - \phi)\sin(\frac{R + r}{R})\hat{\theta} + \cos(\frac{R + r}{R})\hat{\theta}]$$

$$+ \hat{y}[\tan(\alpha - \phi)\cos(\frac{R + r}{R})\hat{\theta} + \sin(\frac{R + r}{R})\hat{\theta}]$$

$$+ r\tan(\alpha - \phi)\cos(\frac{r}{R})\hat{\theta} + R\sin(\frac{r}{R})\hat{\theta} \qquad (2.5.6)$$

Solving equations (2.5.5) and (2.5.6) for $\hat{x}$ and $\hat{y}$, we obtain:

$$\hat{x} = \sin^2(\alpha - \phi)[r\sin\hat{\theta} - R\sin(\frac{r}{R})\hat{\theta}\ \cos(\frac{R + r}{R})\hat{\theta}]$$

$$+ R\sin(\alpha - \phi)\cos(\alpha - \phi)\{\cos(\frac{R + 2r}{R})\hat{\theta} - \sin[\alpha - (\frac{R + r}{R})\hat{\theta}]\}$$

$$+ \cos(\alpha - \phi)^2[r\sin\hat{\theta} + R\cos(\frac{r}{R})\hat{\theta}\ \sin(\frac{R + r}{R})\hat{\theta} - R\sin\alpha\ \sin(\frac{R + r}{R})\hat{\theta}] \qquad (2.5.7)$$

and

$$\hat{y} = \sin^2(\alpha - \phi)[-r\cos\hat{\theta} - R\sin(\frac{r}{R})\hat{\theta}\ \sin(\frac{R + r}{R})\hat{\theta} + R\cos\alpha\ \sin(\frac{R + r}{R})\hat{\theta}]$$

$$+ R\sin(\alpha - \phi)\cos(\alpha - \phi)\{\sin(\frac{R + 2r}{R})\hat{\theta} - \cos[\alpha - (\frac{R + r}{R})\hat{\theta}]\}$$

$$+ \cos(\alpha - \phi)^2[r\cos\hat{\theta} - R\cos(\frac{r}{R})\hat{\theta}\ \cos(\frac{R + r}{R})\hat{\theta} + R\sin\alpha\ \cos(\frac{R + r}{R})\hat{\theta}]$$

Equations (2.5.7) are a pair of parametric equations with $\hat{\theta}$ being the parameter representing the envelope of L relative to G. As described in

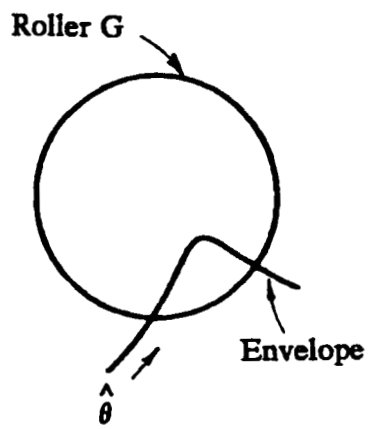

Figure 2.5.2. Tooth Profile of Equation (2.5.7) (R=10, r=2)

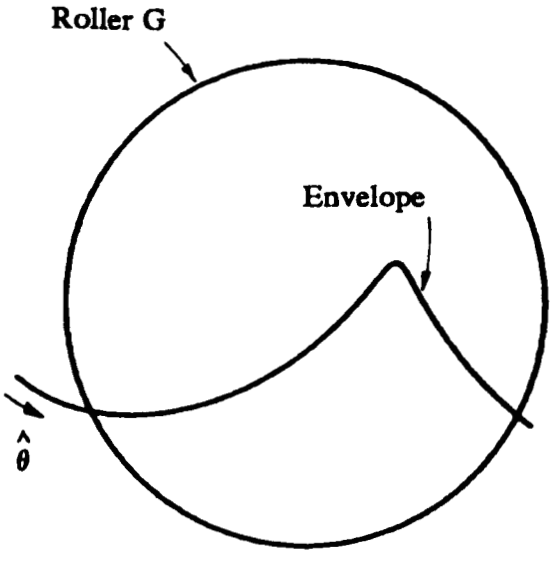

Figure 2.5.3. Tooth Profile of Equation (2.5.7) (R=10, r=10)

Section 3.3, equations (2.5.7) describe the tooth profile impression by the cutter step.

To illustrate the use of equation (3.5.7), the envelope of the straight step on the roller was plotted for $\phi = 20°$. Figure 2.5.2 shows the results for R = 10., r = 2., and $-25. \leq \hat{\theta} \leq 95.$. The circle shown in the figure represents the roller. Figure 2.5.3 shows the envelope for R = 10, r = 10, and $-45. \leq \hat{\theta} \leq 65.$ There is a cusp shown inside the roller. However, only one branch of the envelope is used as the gear tooth.

2.6 Reciprocal Conjugate Gear Tooth and Cutter Profile

In the previous sections, we discussed the analytic expression of the gear tooth profile formed by a given cutter form. It is also of interest to develop an expression for the cutter profile itself for a desired tooth form. This is the "inverse problem".

Consider again a wheel rolling over a step as shown in Figure 2.3.1. Assume the cutter profile is of the form

$$y = f(x) \tag{2.6.1}$$

Substituting equations (2.3.1) and (2.3.2) into (2.6.1), we have:

$$r - \hat{x}\sin\theta + \hat{y}\cos\theta - f(r\theta + \hat{x}\cos\theta + \hat{y}\sin\theta)$$

$$= F(\hat{x}, \hat{y}, \theta) = 0 \tag{2.6.2}$$

$$\frac{\partial F}{\partial \theta} = \hat{x}\cos\theta - \hat{y}\sin\theta - (r - \hat{x}\sin\theta + \hat{y}\cos\theta)f' = 0 \tag{2.6.3}$$

If the cutter's form is known, then by solving equations (2.6.2) and (2.6.3) simultaneously for $\hat{x}$ and $\hat{y}$ as function of θ we obtain the parametric equation of the envelope as:

$$\hat{x} = \hat{x}(\theta)$$

$$\hat{y} = \hat{y}(\theta) \tag{2.6.4}$$

If the cutter's form is unknown, then equations (2.6.2) and (2.6.3) lead to:

$$\frac{df}{dx} = \frac{-\hat{x}\cos\theta - \hat{y}\sin\theta}{r - \hat{x}\sin\theta + \hat{y}\cos\theta} \tag{2.6.5}$$

Suppose the given envelope is in parametric form as in equation (2.6.4). Then substituting into equation (3.6.5) leads to the cutter's profile.

If the given envelope profile is in the form of

$$\hat{y} = g(\hat{x}) \tag{2.6.6}$$

then substituting equations (2.3.1), (2.3.2) and (2.6.5), leads to:

$$x = \psi_1(\hat{x}, \theta) \tag{2.6.7}$$

$$f(x) = \psi_2(\hat{x}, 0) \tag{2.6.8}$$

$$\frac{df}{dx} = \psi_3(\hat{x}, 0) \tag{2.6.9}$$

Solving equations (2.6.7) and (2.5.8), we can obtain the solution for $\hat{x}$ and 0 in terms of x and f(x). Then substituting the results into equation (2.6.9) produces the differential equation for f(x).

To illustrate this procedure, consider equation (2.3.6) in section 2.3 which is the involute profile of the straight cutter. The tooth profile is in the parametric form. Therefore, by substituting equation (2.3.6) into (2.6.5), we have:

$$\frac{df}{dx} = \tan\phi \tag{2.6.10}$$

Integrating equation (2.6.10), it is clear that $y = f(x)$ is a straight line as:

$$f(x) = x\tan\phi + \text{constant} \tag{2.6.11}$$

This is the cutter profile as described in equation (2.3.3).

Chapter 3

Bevel Gear Tooth Surface Generation

3.1 Introduction

Recently, there has been increased interest in the kinematics, stress analysis, dynamic loading, noise, vibration, wear and life of bevel gears--especially spiral bevel gears. This interest has been stimulated by a desire to improve operating and maintenance procedures in high performance transmission of helicopters and other aircraft.

Bevel gears are conical gears, having pitch surfaces in the shape of cones. They are used to connect shafts having intersecting axes. With few exceptions, most bevel gears may be classified as being either of the straight tooth type or of the curved tooth type. The straight tooth gears are called straight bevel gears. The curved tooth gears includes spiral bevel, Zerol bevel, and hypoid gears. Hypoid gears are similar in general form to bevel gears, but operate on axes that are offset.

Spiral Bevel gears used in practice are normally generated with approximately conjugate tooth surfaces by using special machine and tool settings. Therefore, a designer cannot solve the Hertz contact stress problem and define the dynamic capacity and contact fatigue life until these settings are computed. The geometry of the gear tooth surface is very complicated. For example, consider the space width taper and the slot width taper. The space width taper refers to the change in the tooth space width along the tooth length in the pitch plane. Slot width taper refers to the

change in the slot width formed by a V-shaped cutting tool of nominal pressure angle whose sides are tangent to the two sides of the tooth space. The top of the tool is tangent to the root cone along the tooth length in the root plane. The slot width taper is affected by the size of the face mill cutter point width. The productivity of the spiral bevel gear is significantly affected by the size of the cutter point width used to produce it. Experience has shown that a larger point width blade will have longer life than the smaller one [8].

The determination of the principal curvatures and the principal directions of tooth surfaces necessary for calculating the Hertz contact stress is also a difficult problem. It is believed that a quantitative understanding of the geometrical characteristics is fundamental to analyses of the above mentioned physical phenomena of these gears.

The geometrical characteristics and parameters of spiral bevel gears have been documented for some items by the American Gear Manufacturer's Association and others [9-11]. References [12-37] present examples of recent approaches taken to develop a broader understanding of the geometrical characteristics of these gears. For example, Dyson [12] used differential geometry to develop the theory of gearing. Coy [13] described the development of the spiral bevel gear. Bonsignore [8] studied the effect of cutter diameter on the spiral bevel gear tooth proportions. Krenzer [14] studied the effect of the cutter radius on the tooth contact behavior. Litvin, et. al., [15-22] completed works dealing with the theory of spiral bevel gears. Baxter [23-25] completed works dealing with the theory of spiral bevel gears. Baxter [23-25] developed second order surface genera-

tion and discussed the effect of misalignment. Baxter [26] studied the lattice contact with the generated tooth surface. Huston and Coy [27] studied the surface principal radii of curvature of the spiral bevel tooth surface. Suzuki, Kondo, and Ueno [31] investigated cutting condition for improving the cutting efficiency and the roughness of the spiral bevel tooth surface. Huston and Coy [28] analyzed the surface characteristics of the circular cut spiral bevel gear. They presented the analysis of tooth profile changes in the transverse plane of circular cut, spiral bevel crown gears [29]. They also studied the fundamental surface characteristics of spiral bevel gears [30]. Schultes, et. al., [32] presented the CAD/CAM techniques for spiral bevel gears. They also studied the CAD/CAM technique on forging process [33]. Fort [34] developed the inspection system for spiral bevel gears. Uegami, and Tamamura [35] studied the cutter profile. Cloutier, and Gosselin [36] modeled the kinematics error effect of a gear pair. Finally, Winter and Paul [37] measured the tooth root stress of spiral bevel gears.

3.2 Basic Theory

The pitch element is the pitch cone which rolls without slipping at the specified velocity ratio. The pitch element is the instantaneous axis of relative motion of either gear with respect to the other. The two axes and instantaneous axis all lie in the axial plane and intersect at the apex. The base diameters of the pitch cone vary depending upon the gear ratio and the angle between the gear cone axes and the shaft angle. The pitch angle is the angle between the axis and the pitch element.

Figure 3.2.1 illustrates the principal reference planes. The axial plane contains the intersecting axes. The pitch plane is perpendicular to the axial plane and tangent to the pitch cones. The pitch plane and the axial plane intersect in the common pitch element. The transverse plane is perpendicular to the axial plane and the pitch plane.

Figure 3.2.2 illustrates gear axes x_1 and x_2 intersecting at the apex forming the shaft angle Σ. The pitch angles are γ_1 and γ_2. The sum of the pitch angles is the shaft angle.

The crown gear axis x_c lies in the axial plane, and is perpendicular to the pitch element. At a specified cone distance A along the pitch element from the apex is the pitch point P. The distance from the pitch point to the axes are the pitch radii R_1 and R_2. The pitch radii are proportional to the sines of the pitch angles, and their ratio is the velocity ratio.

Formulas relating these quantities and the tooth numbers are listed in Table 3.1.

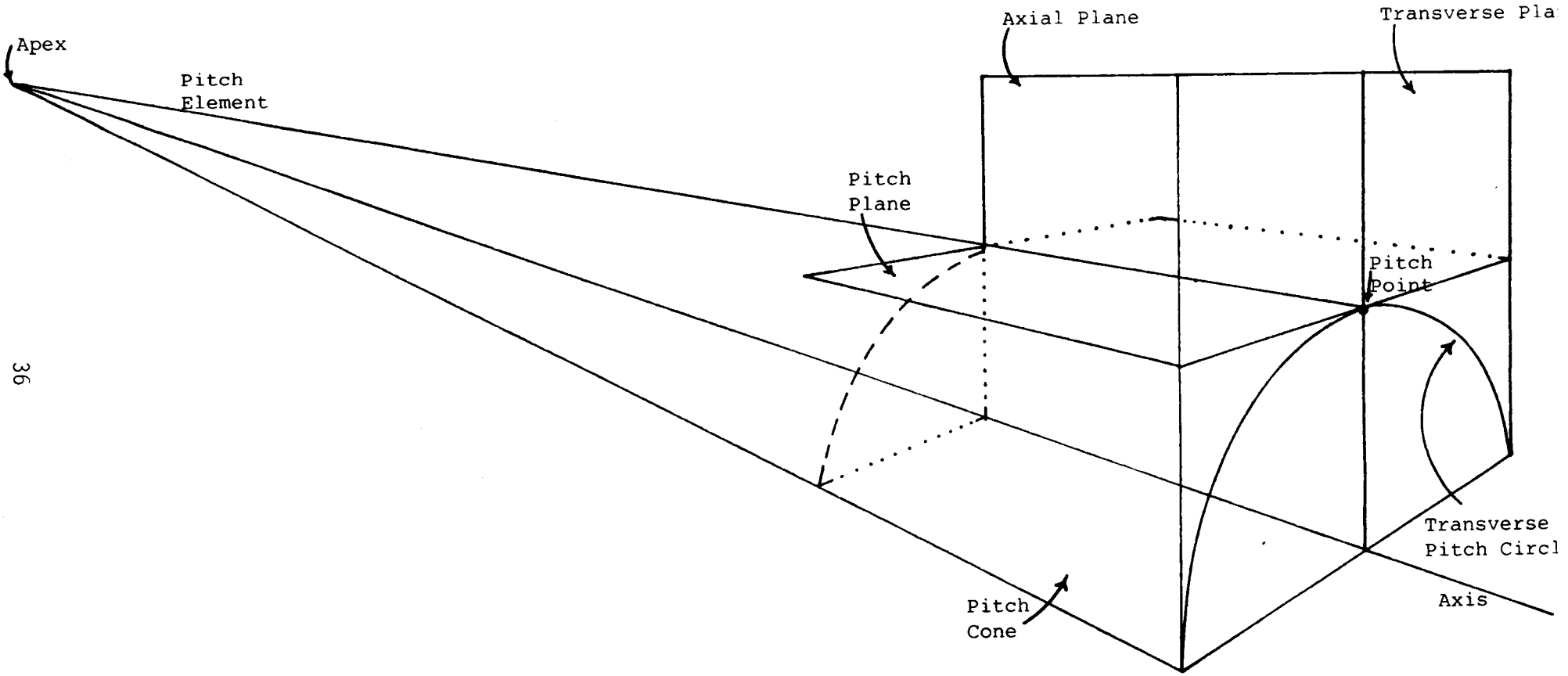

Figure 3.2.1 Reference Planes of a Bevel Gear

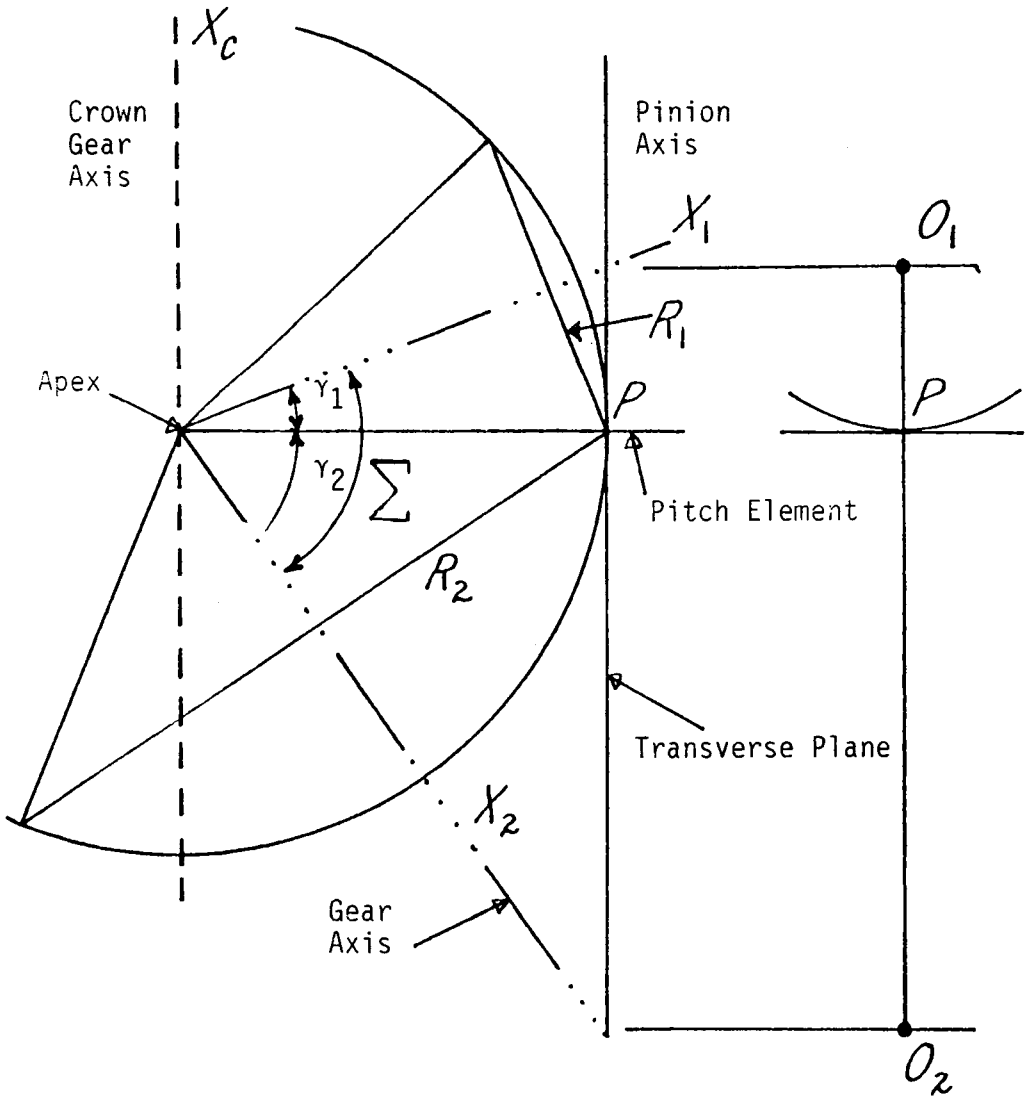

Figure 3.2.2 Axial and Transverse Planes of a Bevel Gear

$$\gamma_1 + \gamma_2 = \Sigma$$

$$w = \frac{N_2}{N_1} = \frac{\sin\gamma_2}{\sin\gamma_1}$$

$$\tan\gamma_1 = \frac{\sin\Sigma}{(w + \cos\Sigma)}$$

$$\tan\gamma_2 = \frac{w \sin\Sigma}{(1 + w\cos\Sigma)}$$

$$N_c = \frac{N_1}{\sin\gamma_1} = \frac{N_2}{\sin\gamma_2}$$

$$R_1 = A \sin\gamma_1$$

$$R_2 = A \sin\gamma_2$$

for $\Sigma = 90°$

$$\tan\gamma_1 = \frac{N_1}{N_2}$$

$$\tan\gamma_2 = \frac{N_2}{N_1}$$

$$A = \sqrt{(R_1^2 + R_2^2)}$$

$$N_c = \sqrt{(N_1^2 + N_2^2)}$$

Table 3.1 Basic Bevel Gear Relations

3.3 Bevel Gear Manufacturing

3.3.1 Bevel Gear Generation and Nongeneration

Two types of machines using the face-mill type of cutter with multiple blades are in general use: generating and nongenerating. The nongenerating type is used for flat gears. The generating type is more universal, and can cut gears with pitch diameters up to 33 inches. The difference between tooth profile by generation and nongeneration is illustrated in Figure 3.3.1 [38]. In the generation operation, the cutter contacts the tooth profile at only one point at a time. In the nongeneration process the cutter makes contact over the entire profile. The gear member of a bevel gear pair has relatively little profile curvature when the tooth ratio is high. In general, the gear is made by a nongenerating roll. The gear member of a nongenerating pair is cut without generation, and the teeth have the shape of the cutter used to cut them. Any necessary compensation for a smooth operation is given on the tooth profile of the mating pinion. The pinion is cut by generation.

The chief advantage of nongenerating gears over generating gears is the economics of production. Since no generating motions are required, a nongenerating pair can be cut several times faster than a generated gear of the same specifications. The cutting time and the equipment used are the same for the pinion member regardless of whether it is cut to operate with a nongenerating or with a generating gear. The nongenerating gears, include Helixform, Formate, Equicurve, and Coniflex gears which are the trade mark of Gleason Works, Rochester, NY. They are cut with the conical face mill cutter. The nongenerating machines are relatively simple com-

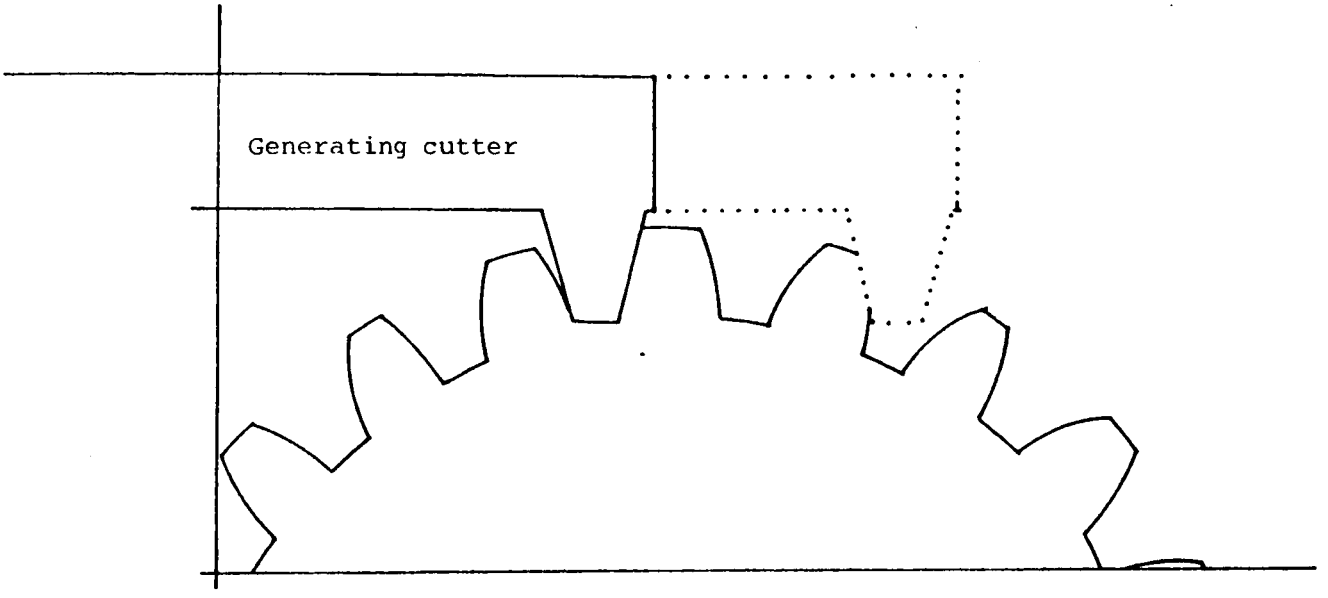

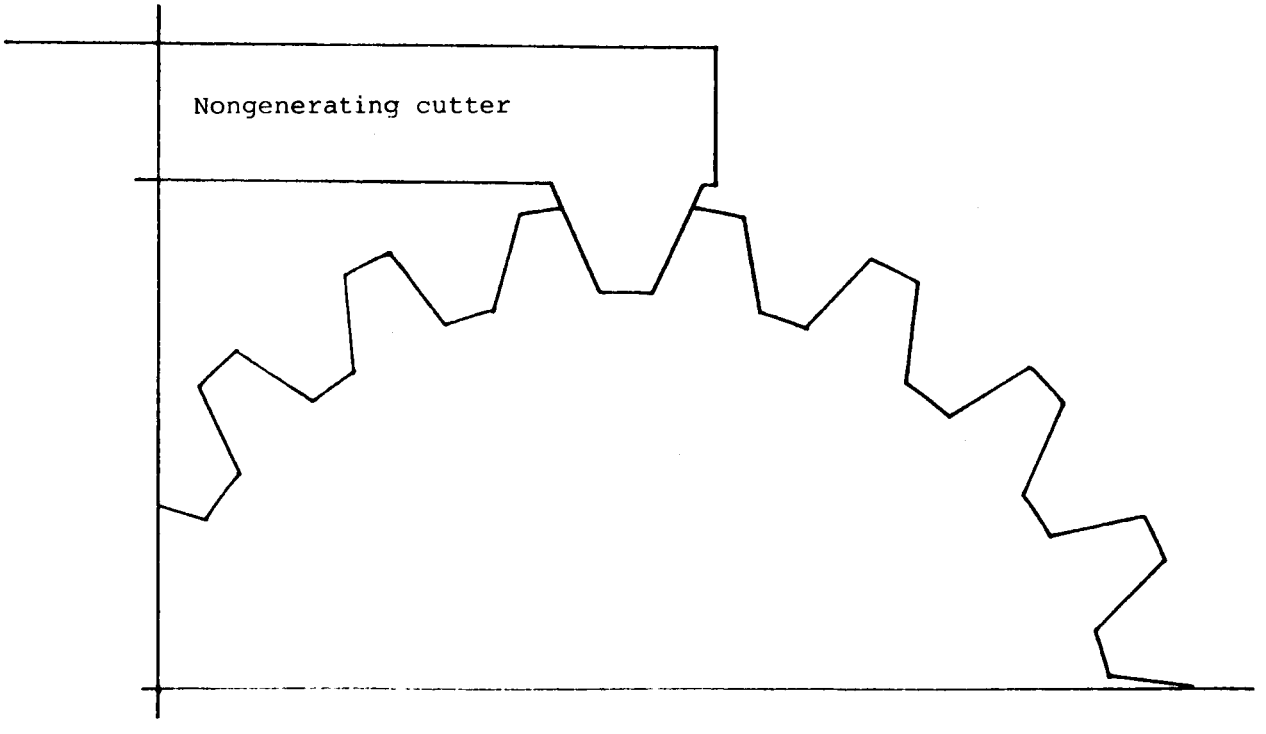

Figure 3.3.1 Generation and Nongeneration

pared with generating machines. Helixform and Formate pairs consist of a nongenerated gear produced by the named method, and a pinion with teeth generated to match.

3.3.2 The Generating Process

Generation can be called the basic process in bevel gear manufacture, because at least one member of every pair must be generated. This is usually the member having the lesser number of teeth, the pinion. The theory of generation involves the following concepts [38]:

1. An imaginary rigid bevel gear called the generating gear. This may be considered as a crown gear, a mating gear, or some other bevel gear.
2. A gear blank or workpiece upon which teeth are to be produced.
3. The positioning of a generating gear and the workpiece so that the teeth of the generating gear are in mesh with the teeth of the workpiece.
4. The turning of the generating gear and workpiece on their respective axes according to a prescribed motion. The turning motion is defined by the imaginary nonslip rolling of the pitch surfaces of the generating gear and workpiece.
5. The envelopment of teeth of the workpiece by the teeth of the generating gear.

In the generating process, the tool simulates one or more teeth of an imaginary generating gear by virtue of its shape and motions. The generating gear may be a basic rack (or crown gear), or it may be the mating gear itself. In general, it may be any gear known to be conjugate to the gear to be produced. The most important requirement for the generating

gear is that it can be readily simulated by a tool with practical mechanical motions. Modern gear cutting machines use straight-sided tooth cutters to generate the gear tooth surfaces. The straight-sided tooth tool is easier to produce and maintain than a profile form tool. Further, by the generation motion, the same cutter can be used to generate profiles for all tooth numbers of the same pitch. The lines of contact between the workpiece and the tool are the same as between the workpiece and the generating gear. The surface generated will be continuous. This type of generation is found in hobbing, grinding, and lapping processes.

3.3.3 The Basic Generator

The production of gear teeth by the generating process requires the following features (See [38]):

1. At least one tooth of the generating gear must be described by the motion of the cutting tool.
2. The workpiece must be positioned relative to the cutting tool to produce meshing between the teeth of the workpiece and the teeth of the generating gear, as they are represented by the cutter.
3. The cutting tool must be carried on a rotating machine member called a "cradle." The axis of the cradle is identical with the axis of the generating gear.
4. The cradle and workpiece rotate on their own axes and they, roll together as a workpiece and imaginary generating gear.
5. A means of indexing must be provided.

Thus the rotating cradle carrying a cutter represents a generating gear rolling with the workpiece. The motion of the cutter simulates the

teeth of the generating gear. As the cutter is carried about the cradle axis, teeth are "enveloped" on the rotating workpiece. The concept of the imaginary generating gear is the key to understanding the generating process. Figure 3.3.2 illustrates the representation of a generating gear by a face-mill cutter on a Gleason hypoid-gear generator [38]. Fundamental design differences that exist among different types of gear generators have originated because of different concepts of the imaginary generating gear.

3.3.4 Spiral Bevel Gear Cutting

Figure 3.3.3 illustrates the configuration of the basic generator of a spiral bevel gear [38]. The cradle carries the cutter, sweeping out the tooth surface. The gear to be cut is held by a rotatable spindle which is part of the work head. The work head is adjustable axially so that gears of different mounting distance can be accommodated. The work head is supported by a swinging base which is rotationally adjustable about a vertical axis. The swinging feature of this base is requried in order to accommodate gears of different pitch angle. Beneath the swinging base is the sliding base. This member is movable and adjustable in a direction parallel to the cradle axis. Adjustment is made in the position of the base to establish the correct depthwise relationship between the cutting tool and the workpiece.

It can also be moved back from the cutting position to obtain clearance for mounting and dismounting the workpiece. The sliding base is supported by the main frame of the machine, which holds a housing supporting the cradle member. Figure 3.3.4 illustrates the spiral bevel pinion being cut on generating type machine [39].

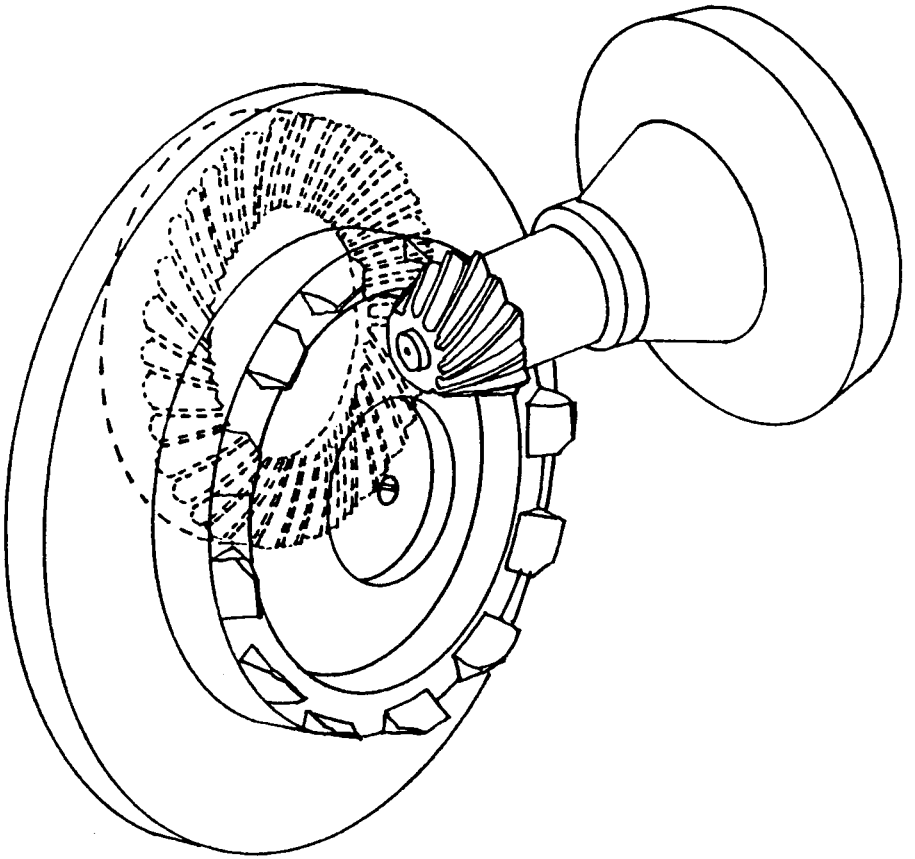

Figure 3.3.2 Face-Mill Cutter Is The Generating Gear

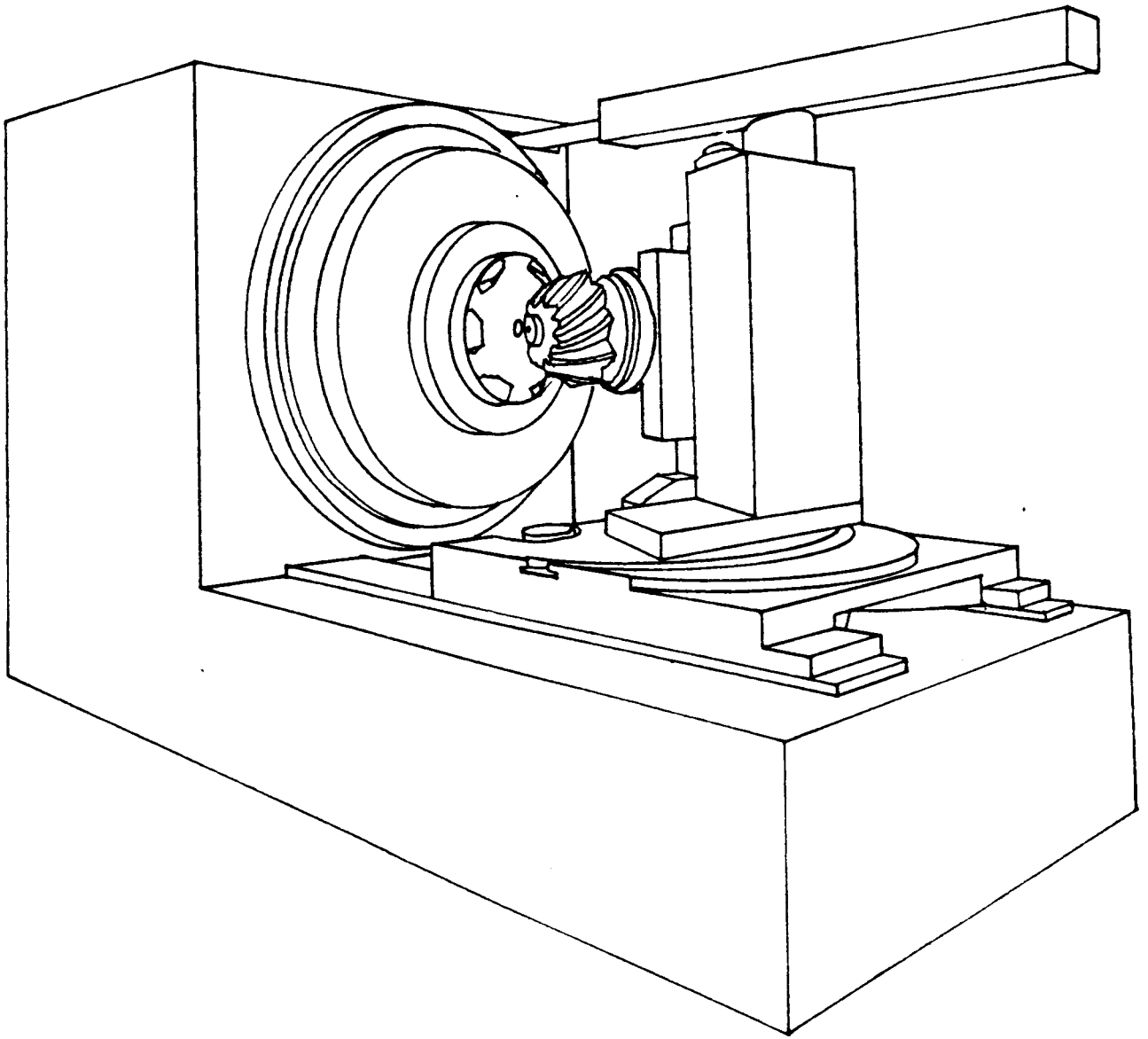

Figure 3.3.3 Arrangement of Bevel Gear Generator

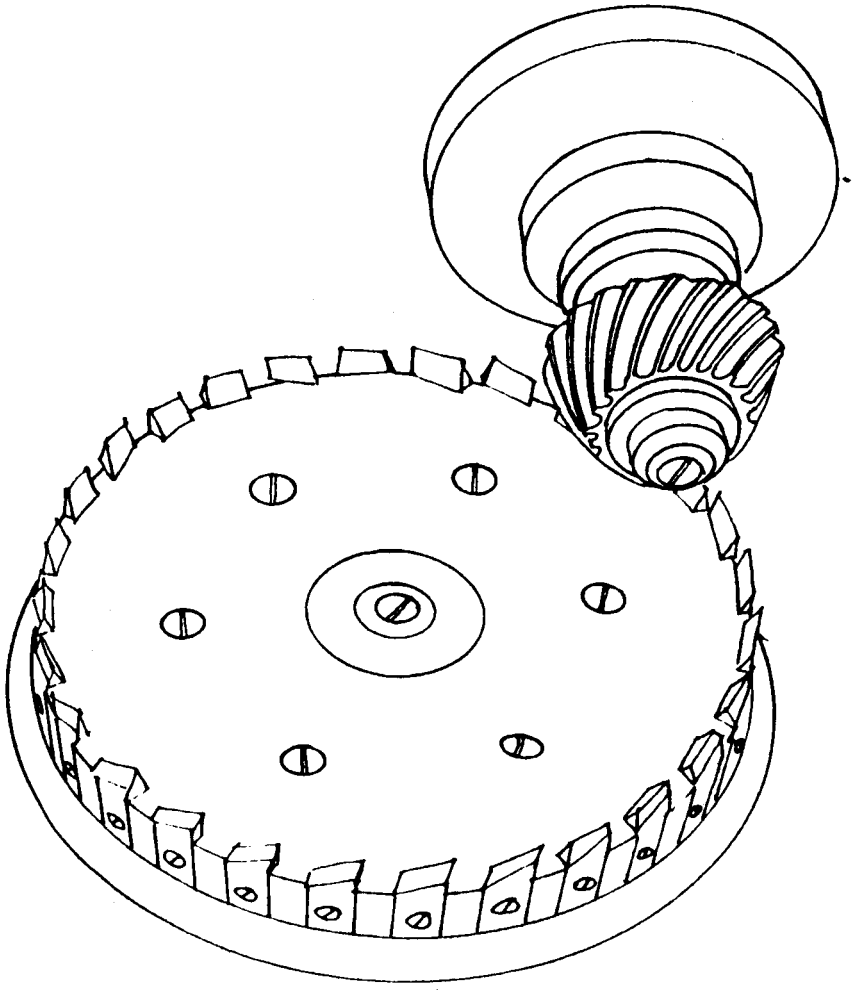

Figure 3.3.4 Spiral Bevel Pinion Being Cut on Generator

The sequence of the operation of a typical bevel gear generator is as follows [38]: The sliding base moves forward to bring the work into engagement with the cutter, and the generating motion of the cradle and workpiece begins (Fig. 3.3.5 A, B). After the operation is completed on a tooth space, the sliding base is moved back (Fig. 3.3.5 C), and the cradle and work spindle reverse their rotation. The cradle returns to its original position, but the work is indexed one tooth during its return roll. The sliding base then moves forward for the start of the next cycle.

3.4 Straight Bevel Gear Tooth Surface Generation

The cutter used for the surface generation of the straight bevel gear tooth is called "the plane basic crown rack." The plane basic crown rack is simply a plane through the machine center. Figure 3.4.1 depicts the machining model of the straight bevel gear tooth generation. The basic crown rack R with the side of an inclined plane is modeled as a "rack step" fixed on an imaginary crown gear pitch plane C. The gear blank G is a cone with the vertex at the machine center O. The gear blank rolls on the crown gear pitch plane C. The crown gear pitch plane is an imaginary fixed plane. When the gear blank rolls over the crown rack step, the envelope of the basic crown rack is the tooth surface of the straight bevel gear.

The coordinate system describing the crown gear is S(X, Y, Z) with origin at O. The coordinate system $\hat{S}(\hat{X}, \hat{Y}, \hat{Z})$ is fixed on the gear blank also with origin at O. The gear blank rotates through an angle θ about $\hat{X}$. The pitch angle of the gear blank is γ. The initial position of the gear blank is defined by the angle α_0 which is the angle between the $\hat{X}$ axis, and

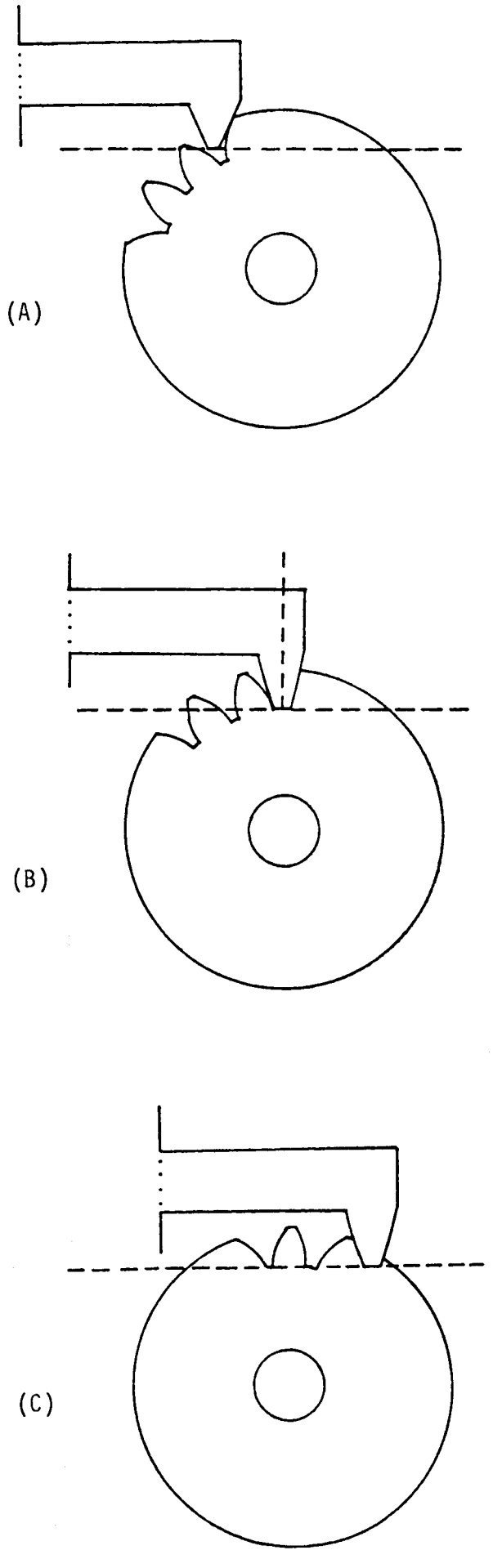

Figure 3.3.5 Bevel Gear Generating Cycle

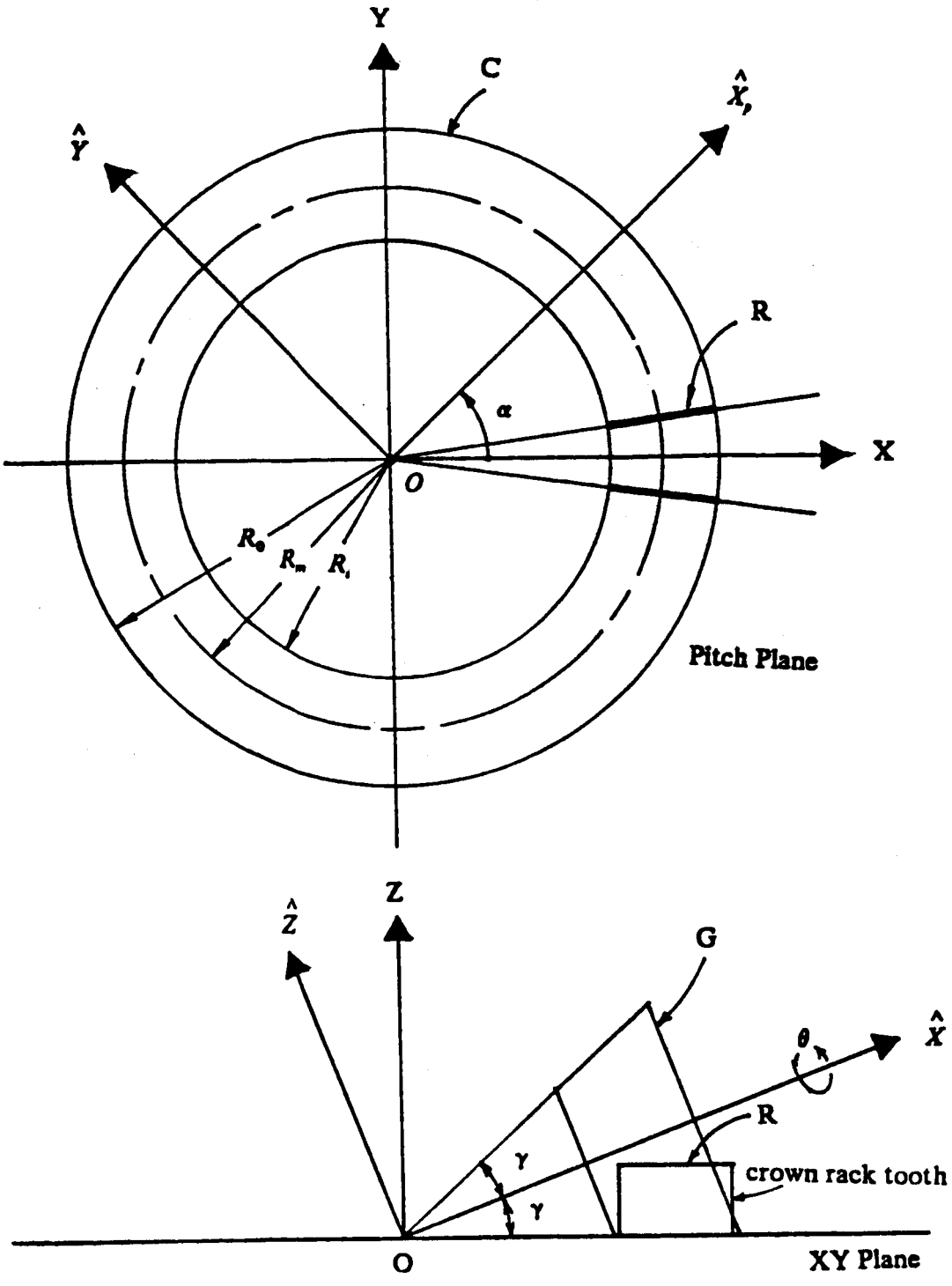

Figure 3.4.1. Straight Bevel Gear Tooth Surface Generation

the projection of the $\hat{X}$ axis on the crown gear pitch plane, denoted by $\hat{X}_p$. During the rolling motion, the angular position of the gear blank is defined by the angle α. Hence, by considering the geometry of the rotation the relation between α and θ is:

$$\alpha = \alpha_0 - \theta\tan\gamma \tag{3.4.1}$$

The coordinate system $\hat{S}$ may be obtained by coordinate transformation from the S as follows:

Step	Axis of rotation	Angle turned	Coordinate system at XYZ initially	Rotation matrix
1	Z	α		R_1
2	Y_1	$-\gamma$	$X_1Y_1Z_1$	R_2
3	X_2	θ	$\hat{X}\hat{Y}\hat{Z}$	R_3

Then the rotation matrices are:

$$[R_1] = \begin{bmatrix} \cos\alpha & -\sin\alpha & 0 \\ \sin\alpha & \cos\alpha & 0 \\ 0 & 0 & 1 \end{bmatrix} \tag{3.4.2}$$

$$[R_2] = \begin{bmatrix} \cos\gamma & 0 & -\sin\gamma \\ 0 & 1 & 0 \\ \sin\gamma & 0 & \cos\gamma \end{bmatrix} \tag{3.4.3}$$

$$[R_3] = \begin{bmatrix} 1 & 0 & 0 \\ 0 & \cos\theta & -\sin\theta \\ 0 & \sin\theta & \cos\theta \end{bmatrix} \tag{3.4.4}$$

Let $\underset{\sim}{r}$ be a position vector locating a point relative to S. Let the components of $\underset{\sim}{r}$ in S have the form:

$$\underset{\sim}{r} = \begin{bmatrix} x \\ y \\ z \end{bmatrix} \tag{3.4.5}$$

Similarly, let $\underset{\sim}{r}_g$ be a position vector locating a point relative to $\hat{S}$. Let the components of $\underset{\sim}{r}_g$ in $\hat{S}$ have the form:

$$\underset{\sim}{r}_g = \begin{bmatrix} \hat{x} \\ \hat{y} \\ \hat{z} \end{bmatrix} \tag{3.4.6}$$

Thus $\underset{\sim}{r}$ and $\underset{\sim}{r}_p$ as given by equations (3.4.5) and (3.4.6), are related by expression:

$$\underset{\sim}{r} = [R_1][R_2][R_3]\underset{\sim}{r}_g = [R]\underset{\sim}{r}_g \tag{3.4.7}$$

[R] may be obtained by using equations (3.4.2), (3.4.3) and (3.4.4). Let r_{ij} (i, j = 1, 3) be components. Hence, we have:

$$\begin{aligned}
r_{11} &= \cos\alpha\cos\gamma \\
r_{12} &= -\cos\alpha\sin\gamma\sin\theta - \sin\alpha\cos\theta \\
r_{13} &= -\cos\alpha\sin\gamma\cos\theta + \sin\alpha\sin\theta \\
r_{21} &= \sin\alpha\cos\gamma \\
r_{22} &= -\sin\alpha\sin\gamma\sin0 + \cos\alpha\cos\theta \\
r_{23} &= -\sin\alpha\sin\gamma\cos0 - \cos\alpha\sin\theta \\
r_{31} &= \sin\gamma \\
r_{32} &= \sin\theta\cos\gamma \\
r_{33} &= \cos0\cos\gamma
\end{aligned} \tag{3.4.8}$$

3.4.1 The Crown Rack

The basic crown rack lies in a plane. It has a straight blade and moves in a reciprocating radial direction. The surface of the rack forms an inclined plane and it passes through the crown gear center. Figure 3.4.2 shows the normal view of the rack profile. Figure 3.4.3 shows the cutter surface in the pitch plane.

The equation of the rack surface may be expressed as:

$$x\tan\psi - y - z\cot\psi = 0 \tag{3.4.9}$$

where ψ is the angle between the cutter plane and the XZ plane. ψ is related to the "tooth angle" [4]. ϕ is the complement of pressure angle of the cutter as shown in Figure 3.4.2. The cutter's surface may be expressed in terms of the gear blank's system $\hat{S}$ by substituting from equations (4.4.7) and (4.4.8) into (4.4.9). This leads to:

$$\begin{aligned}
&\hat{x}[(\tan\psi\cos\alpha - \sin\alpha)\cos\gamma - \cot\phi\sin\gamma] \\
&\quad + \hat{y}[\sin\gamma\sin\theta(\sin\alpha - \tan\psi\cos\alpha) - \cos\theta(\cos\alpha + \tan\psi\sin\alpha) \\
&\quad - \cot\phi\cos\gamma\sin\theta] \\
&\quad + \hat{z}[\sin\gamma\cos\theta(\sin\alpha - \tan\psi\cos\alpha) - \sin\theta(\cos\alpha + \tan\psi\sin\alpha) \\
&\quad - \cot\phi\cos\gamma\cos\theta] \\
&\quad = 0 = F(\hat{x}, \hat{y}, \hat{z}, \theta)
\end{aligned} \tag{3.4.10}$$

To determine the envelope of the cutter surface on the generated gear blank, we simply compute the partial derivative in equation (4.4.10) with respect to the parameter θ (See Appendix A2.). This leads to:

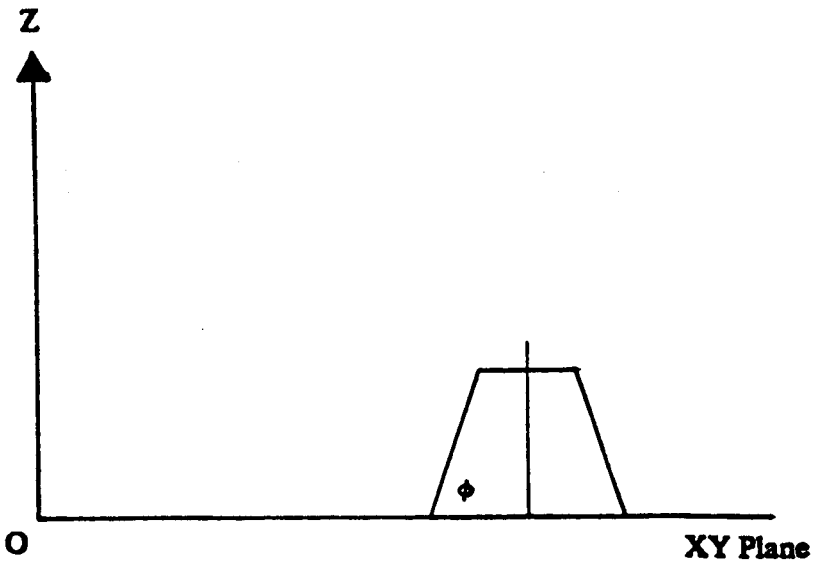

Figure 3.4.2. Normal Plane

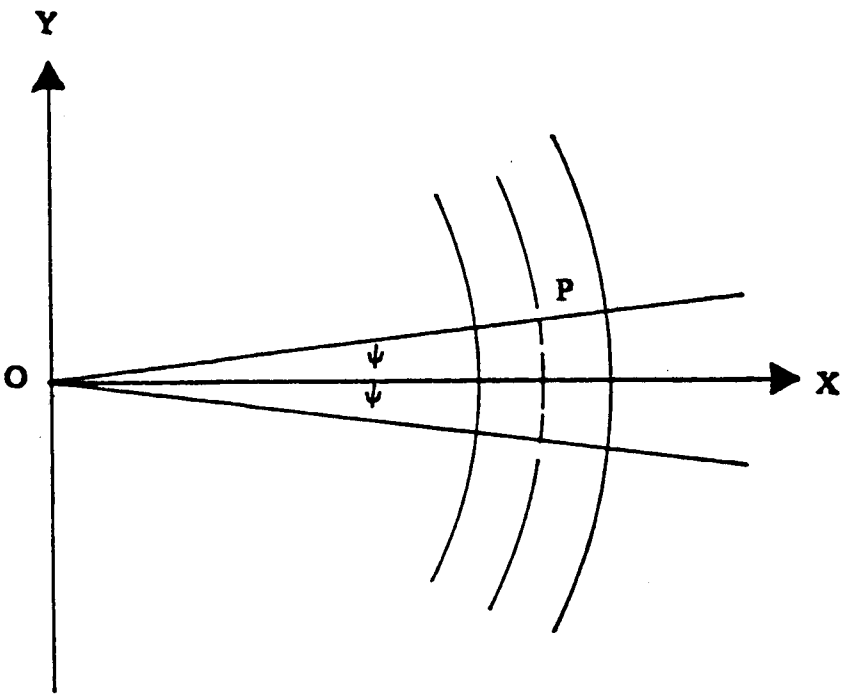

Figure 3.4.3. Pitch Plane

$$\hat{x}[\sin\psi(\tan\psi\sin\alpha + \cos\alpha)]$$
$$+ \hat{y}[\sin\theta(1 - \sin\gamma\tan\gamma)(\cos\alpha + \tan\psi\sin\alpha)$$
$$+ \cos\theta(\sin\gamma - \tan\gamma)(\sin\alpha - \tan\psi\cos\alpha) - \cot\phi\cos\gamma\cos\theta]$$
$$+ \hat{z}\,[\cos\theta(1 - \sin\gamma\tan\gamma)(\cos\alpha + \tan\psi\sin\alpha)$$
$$- \sin\theta(\sin\gamma - \tan\gamma)(\sin\alpha - \tan\psi\cos\alpha) + \cot\phi\cos\gamma\sin\theta]$$
$$= 0 \qquad (3.4.11)$$

During the partial differentiation operation, the terms $\frac{\partial\cos\alpha}{\partial\theta}$ and $\frac{\partial\sin\alpha}{\partial\theta}$ are obtained by using equation (3.4.1).

3.4.2 Straight Bevel Tooth Surface Equation

Equations (3.4.10) and (3.4.11) may be rewritten as:

$$a_1\hat{x} + b_1\hat{y} + c_1\hat{z} = 0 \qquad (3.4.12)$$
$$a_2\hat{x} + b_2\hat{y} + c_2\hat{z} = 0 \qquad (3.4.13)$$

Let $\hat{x}$ be an independent variable, then, from equations (3.4.12) and (3.4.13), $\hat{y}$ and $\hat{z}$ may be determined in terms of $\hat{x}$. Hence, we have:

$$\hat{x} = \hat{x}$$
$$\hat{y} = \frac{a_1b_2 - a_2b_1}{c_1b_2 - c_2b_1}\hat{x}$$
$$\hat{z} = \frac{a_2c_1 - a_1c_2}{c_1b_2 - c_2b_1}\hat{x} \qquad (3.4.14)$$

where the coefficients are:

$$
\begin{aligned}
a_1 &= (\tan\psi\cos\alpha - \sin\alpha)\cos\gamma - \cot\phi\sin\gamma \\
b_1 &= \sin\gamma\sin\theta(\sin\alpha - \tan\psi\cos\alpha) - \cos\theta(\cos\alpha + \tan\psi\sin\alpha) \\
&\quad - \cot\phi\cos\gamma\sin\theta \\
c_1 &= \sin\gamma\cos\theta(\sin\alpha - \tan\psi\cos\alpha) - \sin\theta(\cos\alpha + \tan\psi\sin\alpha) \\
&\quad - \cot\phi\cos\gamma\cos\theta \\
a_2 &= \sin\gamma(\tan\phi\sin\alpha + \cos\alpha) \\
b_2 &= \sin\theta(1 - \sin\gamma\tan\gamma)(\cos\alpha + \tan\psi\sin\alpha) \\
&\quad + \cos\theta(\sin\gamma - \tan\gamma)(\sin\alpha - \tan\psi\cos\alpha) - \cot\phi\cos\gamma\cos\theta \\
c_2 &= \cos\ (1 - \sin\gamma\tan\gamma)(\cos\alpha + \tan\psi\sin\alpha) \\
&\quad - \sin\theta(\sin\gamma - \tan\gamma)(\sin\alpha - \tan\psi\cos\alpha) + \cot\phi\cos\gamma\sin\theta
\end{aligned}
\qquad (3.4.15)
$$

Equation (3.4.14), with coefficients given by equation (3.4.15), represents the envelope of the rack relative to the gear blank. This is the tooth surface of the straight bevel gear. Observe that since the coefficients are function of θ, the tooth surface has the parametric form as:

$$
\begin{aligned}
\hat{x} &= \hat{x} \\
\hat{y} &= \hat{y}(\hat{x}, \theta) \\
\hat{z} &= \hat{z}(\hat{x}, \theta)
\end{aligned}
\qquad (3.4.16)
$$

where $\hat{x}$ and θ are the surface coordinates.

3.5 Spiral Bevel Gear Tooth Surface Generation

3.5.1 Kinematics Relation on the Machine Setting

Figure 3.5.1 depicts a circular cutter generating a spiral bevel gear. The cutter turns about its axis Z_c with an angular rate ω_c. The cutter axis Z_c is fixed in a machine element called the "cradle". The rotating cutter forms a surface which simulates a crown gear. The cradle, and hence the cutter (crown gear surface) also rotate. The rotating axis of the cradle is Z_1, and the rotation rate is ω_g. The rotation rate of the gear blank is ω_p. The cutter has a straight blade. The cutting speed ω_c is independent of ω_g and ω_p. It is not related to the kinematics of tooth generation.

The relation between ω_g and ω_p is

$$\omega_p/\omega_g = N_g/N_p \tag{3.5.1}$$

where N_g and N_p are the numbers of teeth in the crown gear and the generated gear respectively.

The coordinate system used to describe the crown gear is $S_1(X_1, Y_1, Z1)$ with the origin at O_1. The crown gear G with frame S_1 fixed in G rotates through an angle ϕ_1 about Z_1 with respect to a global coordinate system $S_g(X_g, Y_g, Z_g)$ with origin at O_g as in Figure 3.5.1 The System S_g and S_1 have the same origin O_g and O_1. The components of a vector in S_1 may be expressed in terms of the components of a vector in S_g as (See Fig. 3.5.2.):

$$\underline{v}_1 = [R_{1g}]\underline{v}_g \tag{3.5.2}$$

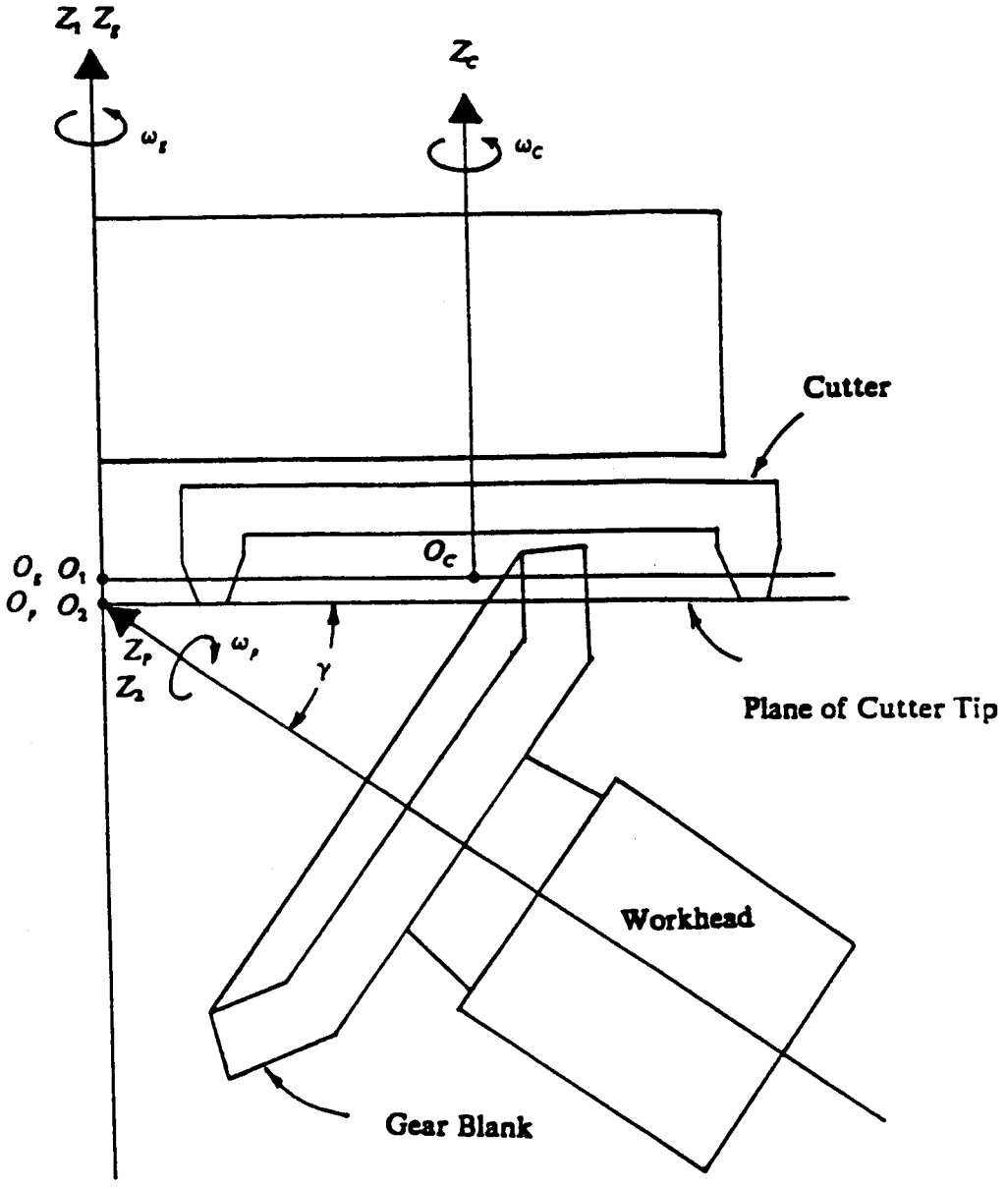

Figure 3.5.1. Machine Setting for Spiral Bevel Gear Manufacturing

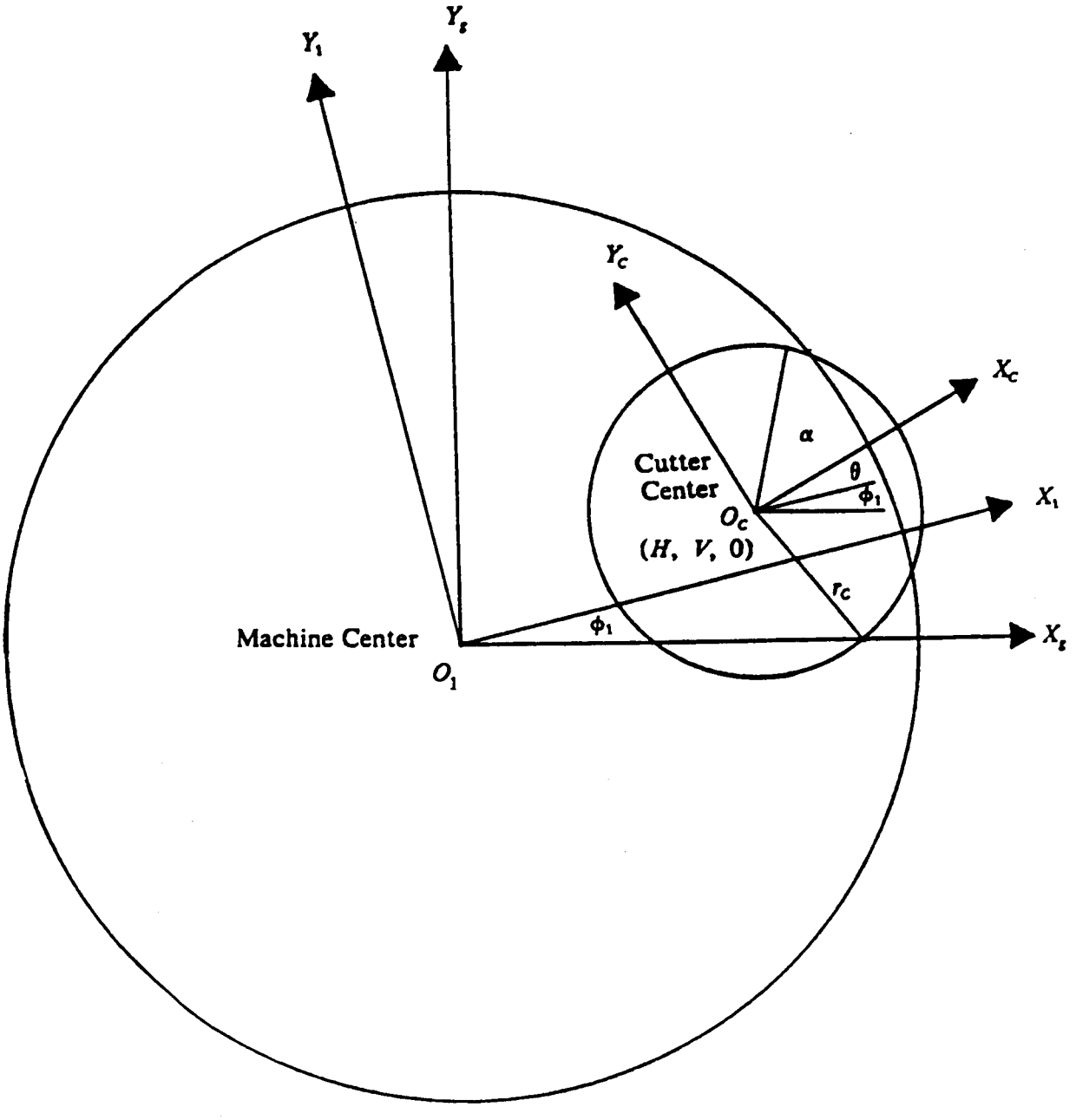

Figure 3.5.2. Relation of Crown Gear and Cutter

where $[R_{1g}]$ is an orthogonal transformation matrix given by

$$[R_{1g}] = \begin{bmatrix} +\cos\phi_1 & \sin\phi_1 & 0 \\ -\sin\phi_1 & \cos\phi_1 & 0 \\ 0 & 0 & 1 \end{bmatrix} \tag{3.5.3}$$

Let $\underset{\sim}{r}_1$ be a position vector locating a point relative to O_1. Let the components of $\underset{\sim}{r}_1$ in S_1 have the form:

$$\underset{\sim}{r}_1 = \begin{bmatrix} x_1 \\ y_1 \\ z_1 \end{bmatrix} \tag{3.5.4}$$

Similarly, let $\underset{\sim}{r}_g$ be a position vector locating a point relative to O_g. Let the components of $\underset{\sim}{r}_g$ in S_g have the form:

$$\underset{\sim}{r}_g = \begin{bmatrix} x_g \\ y_g \\ z_g \end{bmatrix} \tag{3.5.5}$$

Then from equation (4.5.2) $\underset{\sim}{r}_1$ and $\underset{\sim}{r}_g$ are related by the expression:

$$\underset{\sim}{r}_1 = [R_{1g}]\underset{\sim}{r}_g \tag{3.5.6}$$

Let a coordinate system $S_c(X_c, Y_c, Z_c)$ be fixed on the cutter with the origin at $O_c(H, V, 0)$ in the system S_1. H and V are the horizontal and vertical machine settings. (See Fig. 3.5.2.) The cutter rotates through an angle θ about axis Z_c. The coordinate transformation matrix from S_1 to S_c is through $[R_{c1}]$ given by

$$[R_{c1}] = \begin{bmatrix} +\cos\theta & \sin\theta & 0 \\ -\sin\theta & \cos\theta & 0 \\ 0 & 0 & 1 \end{bmatrix} \tag{3.5.7}$$

Let $\underset{\sim}{r}_C$ be a position vector locating a point relative to O_C. Let the components of $\underset{\sim}{r}_C$ in S_C have the form

$$\underset{\sim}{r}_C = \begin{bmatrix} x_C \\ y_C \\ z_C \end{bmatrix} \tag{3.5.8}$$

Then $\underset{\sim}{r}_C$ and $\underset{\sim}{r}_1$, given by equations (3.5.4) and (3.5.8), are related by the expression:

$$\underset{\sim}{r}_1 = [R_{1C}]\underset{\sim}{r}_C + \underset{\sim}{I}_{1C}$$

or

$$\underset{\sim}{r}_C = [R_{C1}]\underset{\sim}{r}_1 + [R_{C1}]\underset{\sim}{I}_{1C} \tag{3.5.9}$$

where $[R_{1C}]$ is the transpose of $[R_{C1}]$, and $\underset{\sim}{I}_{1C}$ is given by the expression:

$$\underset{\sim}{I}_{1C} = \begin{bmatrix} +H \\ +V \\ 0 \end{bmatrix} \tag{3.5.10}$$

Let a coordinate system $S_2(X_2, Y_2, Z_2)$ be fixed in the gear blank. Let S_2 rotate through an angle ϕ_2 about Z_2 with respect to a second global coordinate system $S_p(X_p, Y_p, Z_p)$. See Figure 3.5.1, 3.5.3 and 3.5.5. Observe that S_2 and S_p have the same origin. Also Z_2 coincides with Z_p. The coordinate transformation matrix from S_2 to S_p is $[R_{p2}]$ given by

$$[R_{p2}] = \begin{bmatrix} \cos\phi_2 & -\sin\phi_2 & 0 \\ \sin\phi_2 & +\cos\phi_2 & 0 \\ 0 & 0 & 1 \end{bmatrix} \tag{3.5.11}$$

Let $\underset{\sim}{r}_p$ be a position vector locating a point relative to O_p, the origin of S_p. Let the components of $\underset{\sim}{r}_p$ in S_p have the form:

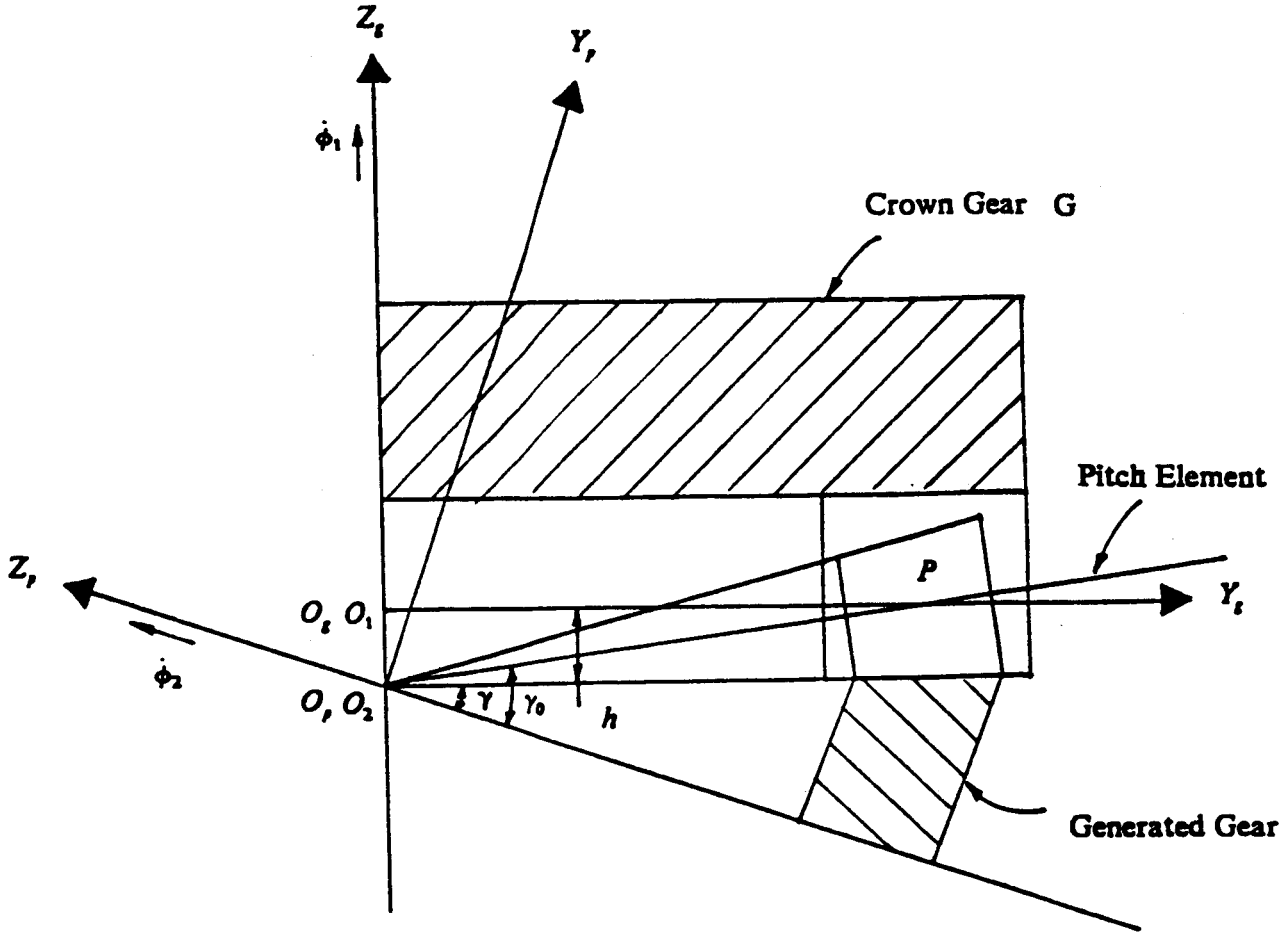

Figure 3.5.3. Relation of Generating Gear and Generated Gear

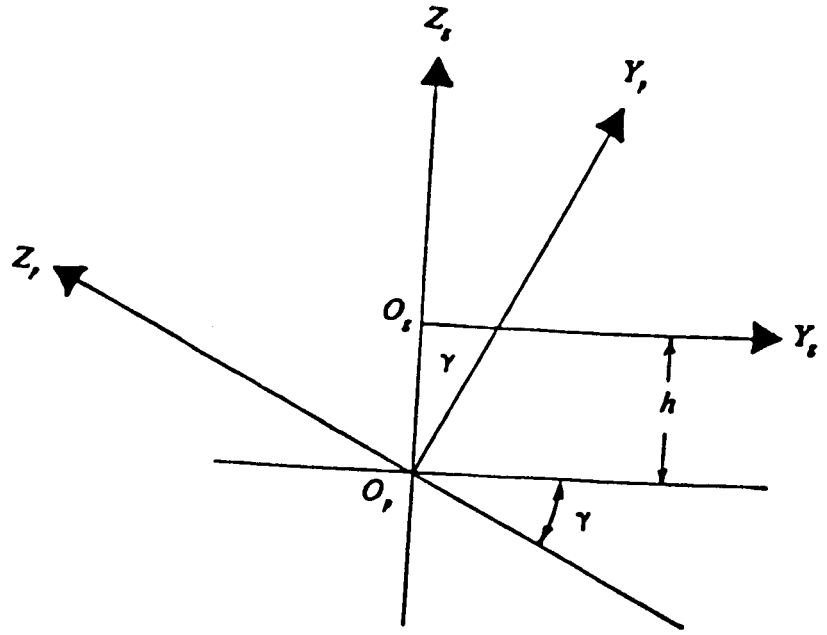

Figure 3.5.4. Relation of System S_g and S_p

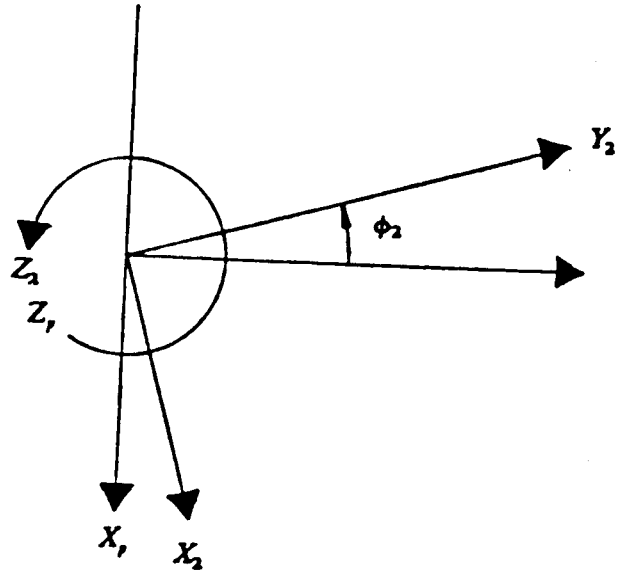

Figure 3.5.5. Relation of System S_p and S_2

$$\underset{\sim}{r}_p = \begin{bmatrix} x_p \\ y_p \\ z_p \end{bmatrix} \tag{3.5.12}$$

Similarly, let $\underset{\sim}{r}_2$ be a position vector locating a point relative to O , the origin of S_2. Let the components of $\underset{\sim}{r}_2$ in S_2 have the form:

$$\underset{\sim}{r}_2 = \begin{bmatrix} x_2 \\ y_2 \\ z_2 \end{bmatrix} \tag{3.5.13}$$

Then $\underset{\sim}{r}_p$ and $\underset{\sim}{r}_2$ are related by the expression:

$$\underset{\sim}{r}_p = [R_{p2}]\underset{\sim}{r}_2 \tag{3.5.14}$$

The two global coordinate systems S_g and S_p are related by the root angle γ of the generated gear and the addendum of the cutter tooth h by transformation equation. See Figure 3.5.1, 3.5.3, and 3.5.4. Hence, $\underset{\sim}{r}_g$ and $\underset{\sim}{r}_p$ are related by the expression:

$$\underset{\sim}{r}_g = [R_{gp}]\underset{\sim}{r}_p + \underset{\sim}{T}_{gp} \tag{3.5.15}$$

where

$$[R_{gp}] = \begin{bmatrix} 1 & 0 & 0 \\ 0 & \sin\gamma & -\cos\gamma \\ 0 & \cos\gamma & +\sin\gamma \end{bmatrix} \tag{3.5.16}$$

and

$$\underset{\sim}{T}_{gp} = \begin{bmatrix} 0 \\ 0 \\ -h \end{bmatrix} \tag{3.5.17}$$

The angular speeds of the crown gear and the generated gear may be expressed in terms of ϕ_1 and ϕ_2 as:

$$\omega_g = \dot{\phi}_1 \tag{3.5.18}$$

$$\omega_p = \dot{\phi}_2 \tag{3.5.19}$$

where the overdot denotes the derivative with respect to time.

During the process of cutting, the simulated crown gear rotates in such a way that the motion is conjugate to the generated gear blank. In Figure 3.5.3, the pitch element O_2P is an instantaneous axis for these "conjugate gears." Hence, their angular velocity components on the pitch element should be equal, that is,

$$\dot{\phi}_2 \sin\gamma_0 = \dot{\phi}_1 \cos(\gamma_0 - \gamma) \tag{3.5.20}$$

where γ_0 is the pitch angle.

Integrating equation (3.5.20) with respect to time, then leads to the relation:

$$\phi_1 = \frac{\sin\gamma_0}{\cos(\gamma_0 - \gamma)} \phi_2 + \phi_{10} \tag{3.5.21}$$

where ϕ_{10} is a constant determined by initial conditions.

Let the constant w be defined as:

$$w = \frac{\sin\gamma_0}{\cos(\gamma_0 - \gamma)} \tag{3.5.22}$$

Equations (3.5.20) and (3.5.21) may be rewritten as:

$$\dot{\phi}_1 = w\dot{\phi}_2 \tag{3.5.23}$$

$$\phi_1 = w\phi_2 + \phi_{10} \tag{3.5.24}$$

Combining equations (3.5.1), (3.5.18), (3.5.19) and (3.5.23) gives the relation:

$$\frac{N_g}{N_p} = \frac{\omega_p}{\omega_g} = \frac{\phi_2}{\phi_1} = \frac{1}{w} \tag{3.5.25}$$

We can see that the magnitude of constant w is the reciprocal of the speed ratio ϕ_2/ϕ_1.

3.5.2 Circular Cutter Surface

Figure 3.5.6 depicts a cutter with a straight blade rotating about the cutter axis Z_c. The straight blade of the cutter describes a conical surface of revolution with vertex angle $(\pi - 2\psi_o)$. The mean radius of the head cutter measured in the plane $Z_c = 0$ is r_c. The apex of the cone is at V ith coordinate $(0, 0, Z_o)$ in S_c. The coordinates (x_c, y_c, z_c) of an arbitrary point C on the surface of revolution can then be obtained by the equations:

$$\begin{aligned} x_c &= (z_o - z_c)\cot\psi_o \cos\alpha \\ y_c &= (z_o - z_c)\cot\psi_o \sin\alpha \end{aligned} \tag{3.5.26}$$

or

$$x_c^2 + y_c^2 = (z_o - z_c)^2 \cot^2\psi_o \tag{3.5.27}$$

where z_c and α are surface coordinates.

Equation (3.5.27) also may be written in the form

$$f(x_c, y_c, z_c) = \tan^2\psi_o(x_c^2 + y_c^2) - (z_o - z_c)^2 = 0 \tag{3.5.28}$$

The cutter surface may be expressed in the gear blank system S_2 by substituting from equations (4.5.9), (4.5.14), (4.5.15) into equation (4.5.6). This leads to:

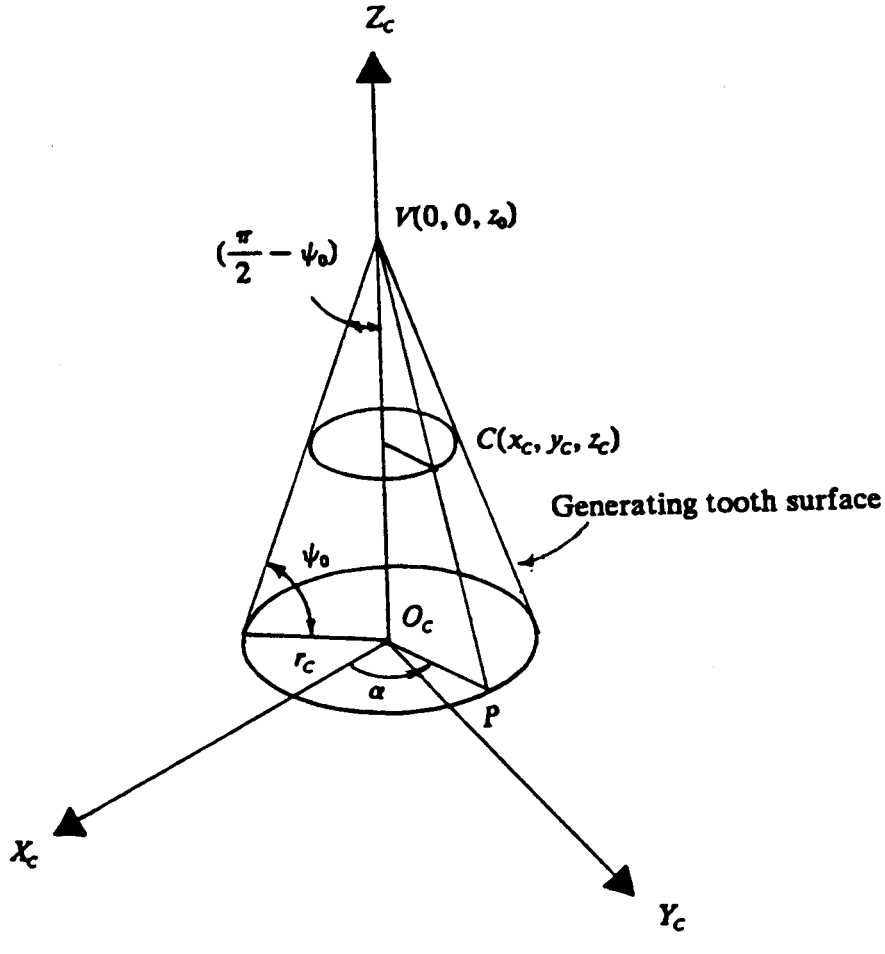

Figure 3.5.6. Surface of Revolution of the Cutter

$$\underset{\sim}{r}_c = [R_{c1}][R_{1g}][R_{gp}][R_{p2}]\underset{\sim}{r}_2 + [R_{c1}][R_{1g}]\underset{\sim}{T}_{gp} + [R_{c1}]\underset{\sim}{T}_{1c}$$

$$= [E]\underset{\sim}{r}_2 + \underset{\sim}{T} \qquad (3.5.29)$$

where [E] and $\underset{\sim}{T}$ are defined as:

$$[E] = [e_{ij}] = [R_{c1}][R_{1g}][R_{gp}][R_{p2}] \qquad (3.5.30)$$

and

$$\underset{\sim}{T} = \underset{\sim}{t}_i = [R_{c1}][R_{1g}]\underset{\sim}{T}_{gp} + [R_{c1}]\underset{\sim}{T}_{1c} \qquad (3.5.31)$$

where i, j = 1, 2, 3.

By substituting from equations (3.5.3), (3.5.7), (3.5.10), (3.5.16) and (3.5.17) into equations (3.5.30) and (3.5.31), the elements of [E] and $\underset{\sim}{T}$, e_{ij} and t_i(i, j = 1, 2, 3) are found to be:

$$e_{11} = \cos\phi_2\cos(\theta + \phi_1) + \sin\gamma\sin\phi_2\sin(\theta + \phi_1)$$

$$e_{12} = -\sin\phi_2\cos(\theta + \phi_1) + \sin\gamma\cos\phi_2\sin(\theta + \phi_1)$$

$$e_{13} = -\cos\gamma\sin(\theta + \phi_1)$$

$$e_{21} = -\cos\phi_2\sin(\theta + \phi_1) + \sin\gamma\sin\phi_2\cos(\theta + \phi_1)$$

$$e_{22} = \sin\phi_2\sin(\theta + \phi_1) + \sin\gamma\cos\phi_2\cos(\theta + \phi_1)$$

$$e_{23} = -\cos\gamma\cos(\theta + \phi_1)$$

$$e_{31} = \cos\gamma\sin\phi_2$$

$$e_{32} = \cos\gamma\cos\phi_2$$

$$e_{33} = \sin\gamma \qquad (3.5.32)$$

and

$$t_1 = +H\cos\theta + V\sin\theta$$

$$t_2 = -H\sin\theta + V\cos\theta$$

$$t_3 = -h \qquad (3.5.33)$$

Hence, the cutter surface expressed in the S_2 coordinate system may be obtained by substituting equations (3.5.29), (3.5.32) and (3.5.33) into equation (3.5.26):

$$\begin{aligned} &e_{11}x_2 + e_{12}y_2 + e_{13}z_2 + t_1 \\ &\quad = [z_0 - (e_{31}x_2 + e_{32}y_2 + t_3)]\cot\psi_0\cos\alpha \\ &e_{21}x_2 + e_{22}y_2 + e_{23}z_2 + t_2 \\ &\quad = [z_0 - (e_{31}x_2 + e_{32}y_2 + r_{33}z_2 + t_3)\cot\psi_0\sin\alpha \end{aligned} \qquad (3.5.34)$$

Alternatively, these expression may be written in the form:

$$\begin{aligned} &(e_{11}\tan\psi_0 + e_{31}\cos\alpha)x_2 + (e_{12}\tan\psi_0 + e_{32}\cos\alpha)y_2 \\ &+ (e_{13}\tan\psi_0 + e_{33}\cos\alpha)z_2 = (z_0 - t_3)\cos\alpha - t_1\tan\psi_0 \end{aligned}$$

and

$$\begin{aligned} &(e_{21}\tan\psi_0 + e_{31}\sin\alpha)x_2 + (e_{12}\tan\psi_0 + e_{32}\sin\alpha)y_2 \\ &+ (e_{13}\tan\psi_0 + e_{33}\sin\alpha)z_2 = (z_0 - t_3)\sin\alpha - t_2\tan\psi_0 \end{aligned} \qquad (3.5.35)$$

3.5.3 Spiral Bevel Gear Tooth Surface Equation

Equations (3.5.35) represent the generating surface seen by the gear blank. To determine the envelope of the cutter surface on the gear blank, we compute the partial derivative of $\underset{\sim}{r}_c$, in equation (4.5.29), with respect to the parameter ϕ_2 (See Appendix A2.). That is:

$$\frac{\partial \underset{\sim}{r}_c}{\partial \phi_2} = \left[\frac{\partial E}{\partial \phi_2}\right]\underset{\sim}{r}_2 + [E]\frac{\partial \underset{\sim}{r}_2}{2} + \frac{\partial T}{\partial \phi_2} \qquad (3.5.36)$$

The second term is zero since $\underset{\sim}{r}_2$ is fixed in S_2. The first and the last terms may be determined from the previous transformation equation--specifically, from equations (3.5.30), and (3.5.32). Let the matrix [D] be defined as:

$$[D] = [d_{ij}] = [\frac{\partial E}{\partial \phi_2}] = [\frac{\partial e_{ij}}{\partial \phi_2}] \tag{3.5.37}$$

The components of [D] may be obtained from equation (3.5.32) as:

$$\begin{aligned}
d_{11} &= -\sin\phi_2\cos(\theta + \phi_1)(1 - w\sin\gamma) + (\sin\gamma - w)\cos\phi_2\sin(\theta + \phi_1) \\
d_{12} &= -\cos\phi_2\cos(\theta + \phi_1)(1 - w\sin\gamma) - (\sin\gamma - w)\sin\phi_2\sin(\theta + \phi_1) \\
d_{13} &= -w\cos\gamma\cos(\theta + \phi_1) \\
d_{21} &= \sin\phi_2\sin(\theta + \phi_1)(1 - w\sin\gamma) + (\sin\gamma - w)\cos\phi_2\cos(\theta + \phi_1) \\
d_{22} &= \cos\phi_2\sin(\theta + \phi_1)(1 - w\sin\gamma) - (\sin\gamma - w)\sin\phi_2\cos(\theta + \phi_1) \\
d_{23} &= -w\cos\gamma\sin(\theta + \phi_1) \\
d_{31} &= \cos\gamma\cos\phi_2 \\
d_{32} &= -\cos\gamma\sin\phi_2 \\
d_{33} &= 0
\end{aligned} \tag{3.5.38}$$

From equations (3.5.31) and (3.5.33), define the vector B as:

$$\underset{\sim}{B} = \underset{\sim}{b}_i = \frac{\partial}{\partial \phi_2}\ \underset{\sim}{T} = \frac{\partial}{\partial \phi_2}\ \underset{\sim}{t}_i \qquad (i = 1, 2, 3) \tag{3.5.39}$$

then

$$b_i = 0 \qquad (i = 1, 2, 3) \tag{3.5.40}$$

Hence, equation (3.5.36) may be rewritten in the form:

$$\frac{\partial}{\partial \phi_2}\ \underset{\sim}{r}_c = [d_{ij}]\underset{\sim}{r}_2 \qquad (i, j = 1, 2, 3) \tag{3.5.41}$$

Equation (3.5.41) represents the derivative of the equation of the transformation from the cutter's system to gear blank system. It is useful for the derivation of the constraint equation of the cutter's motion.

The derivative of the cutter conical surface with respect to ϕ_2, the rotation angle of the gear blank, is (See equation (3.5.28)):

$$\frac{\partial}{\partial\phi_2} f(x_c, y_c, z_c) = 2\tan^2\psi_o(x_c\frac{\partial x_c}{\partial\phi_2} + y_c\frac{\partial y_c}{\partial\phi_2}) + \\ + 2(z_o - z_c)\frac{\partial z_c}{\partial\phi_2} = 0 \qquad (3.5.42)$$

Substituting equation (3.5.26) into (3.5.42), this gives

$$2\tan^2\psi_o[(z_o - z_c)\cot\psi_o\cos\frac{\partial x_c}{\partial\phi_2} \\ + (z_o - z_c)\cot\psi_o\sin\frac{\partial x_c}{\partial\phi_2}] + 2(z_o - z_c)\frac{\partial z_c}{\partial\phi_2} = 0 \qquad (3.5.43)$$

If z_c is not equal to z_o, this becomes:

$$\tan_o[\cos\frac{x_c}{2} + \sin\frac{y_c}{2}] + \frac{z_c}{2} = 0 \qquad (3.5.44)$$

From equation (3.5.41), it is seen that

$$\frac{\partial x_c}{\partial\phi_2} = d_{11}x_2 + d_{12}y_2 + d_{13}z_2$$
$$\frac{\partial y_c}{\partial\phi_2} = d_{21}x_2 + d_{22}y_2 + d_{23}z_2$$
$$\frac{\partial z_c}{\partial\phi_2} = d_{31}x_2 + d_{32}y_2 + d_{33}z_2 \qquad (3.5.45)$$

Substituting equation (3.5.45) into (3.5.44), then leads to:

$$\tan\psi_o[\cos\alpha(d_{11}x_2 + d_{12}y_2 + d_{13}z_2) \\ + \sin\alpha(d_{21}x_2 + d_{22}y_2 + d_{23}z_2)] \\ + (d_{31}x_2 + d_{33}z_2) = 0 \qquad (3.5.46)$$

or

$$[\tan\psi_o(d_{11}\cos\alpha + d_{21}\sin\alpha) + d_{31}]x_2 \\ + [\tan\psi_o(d_{21}\cos\alpha + d_{22}\sin\alpha) + d_{32}]y_2 \\ + [\tan\psi_o(d_{13}\cos\alpha + d_{23}\sin\alpha) + d_{33}]z_2 \\ = 0 \qquad (3.5.47)$$

Equation (3.5.47) is the constraint equation of the cutter motion on the gear blank. Combining equations (3.5.35) and (3.5.47), then leads to the equation

$$a_{11}x_2 + a_{12}y_2 + a_{13}z_2 = a_{14}$$

$$a_{21}x_2 + a_{22}y_2 + a_{23}z_2 = a_{24}$$

$$a_{31}x_2 + a_{32}y_2 + a_{33}z_2 = a_{34} \qquad (3.5.48)$$

where coefficients $a_{ij}(i, j = 1, 3)$ are:

$$a_{11} = e_{11}\tan\psi_o + e_{31}\cos\alpha$$

$$a_{12} = e_{12}\tan\psi_o + e_{32}\cos\alpha$$

$$a_{13} = e_{13}\tan\psi_o + e_{33}\cos\alpha$$

$$a_{14} = (z_o - t_3)\cos\alpha - t_1\tan\psi_o$$

$$a_{21} = e_{21}\tan\psi_o + e_{31}\sin\alpha$$

$$a_{22} = e_{22}\tan\psi_o + e_{32}\sin\alpha$$

$$a_{23} = e_{23}\tan\psi_o + e_{33}\sin\alpha$$

$$a_{24} = (z_o - t_3)\sin\alpha - t_2\tan\psi_o$$

$$a_{31} = \tan\psi_o(d_{11}\cos\alpha + d_{21}\sin\alpha) + d_{31}$$

$$a_{32} = \tan\psi_o(d_{12}\cos\alpha + d_{22}\sin\alpha) + d_{32}$$

$$a_{33} = \tan\psi_o(d_{13}\cos\alpha + d_{23}\sin\alpha) + d_{33}$$

$$a_{34} = 0$$

Equation (3.5.48) with coefficients from equation (3.5.49) forms a set of simultaneous equations representing the envelope of the cutter relative to the gear blank. The solution of equation (3.5.41) describes the tooth surface impression created by the cutter. Observe that since the coefficients a_{ij} are functions of (α, ψ_1), the solution of equation (3.5.48) has the parametric form:

$$x_2 = x_2(\alpha, \phi_1)$$

$$y_2 = y_2(\alpha, \psi_1)$$

$$z_2 = z_2(\alpha, \phi_1) \qquad (3.5.50)$$

where α and ϕ_1 are the surface coordinates.

Chapter 4

Conclusions and Applications

A new modeling method simulating the gear manufacturing process has been presented. The method is applicable with hobbing and shaping procedures. It can be used with both spur and bevel gears.

The model simulates the kinematics of the gear cutter. The cutter profile is described in terms of the gear blank coordinate system. Applying a one parameter envelope theory, with the rotation angle of the gear blank being the parameter, the envelope of the cutter profile on the gear blank describes the gear tooth profile. The partial derivative of the cutter equation with respect to the rotation angle, determines the constraint equation of the cutter motion. The simultaneous solution of the cutter equation and cutter constraint equation provides the cutter envelope which is the gear tooth profile. These are equations (2.3.6), (2.4.4) and (2.4.5) of Chapter 2 for standard and nonstandard gear tooth profiles, and equation (3.4.16) of Chapter 3 for straight bevel gear tooth surfaces, and equation (3.5.50) of Chapter 3 for spiral bevel gear tooth surfaces. The gear shaping simulation is modeling in Section 2.5. The cutter takes the rack form on a wheel. The shaped gear tooth profile is expressed in equation (2.5.7).

There are many applications of the foregoing analysis. It may be used to study straight and spiral bevel gear tooth surface characteristics. The effects of the machine settings, the cutter radius, the mean cone distance,

tooth space width taper, and slot width taper [8] can also be examined. Also, the surface equations of the bevel gear tooth may be accurately digitized for a finite element mesh generation. Finally, the static and dynamic analysis of these gears may be studied.

Future efforts should include extending these procedures to study gears with non-intersecting shafts--that is, hypoid gears. Also, software to automatically generate these gear tooth surfaces needs to be developed. The effect of surface characteristics on the stresses, performance, and life needs to be examined. Finally, the use of these procedures for optimal design needs to be developed.

Appendix A1. The Envelope of a Family of Curves

In the xy plane, let

$$F(x, y, t) = 0 \tag{A1}$$

be the equation of a family of curves. Let E be a curve in the plane tangent to each curve of the family. Let t be a parameter for the envelope and let

$$x = x(t), \quad \text{and} \quad y = y(t) \tag{A2}$$

Since these relations make equation (A1) an identity, we have

$$\frac{\partial F}{\partial x}\frac{dx}{dt} + \frac{\partial F}{\partial y}\frac{dy}{dt} + \frac{\partial F}{\partial t} = 0 \tag{A3}$$

On any given curve, t is constant. Hence, we have the equation

$$\frac{\partial F}{\partial x} + \frac{\partial F}{\partial y}\frac{dy}{dx} = 0 \tag{A4}$$

This determines the slope of E at any point. Hence

$$\frac{dy}{dx} = \frac{dy/dt}{dx/dt}$$

and

$$\frac{\partial F}{\partial x}\frac{dx}{dt} + \frac{\partial F}{\partial y}\frac{dy}{dt} = 0 \tag{A5}$$

A comparison of equations (A3) and (A5) shows that:

$$\frac{\partial F}{\partial t} = 0 \tag{A6}$$

This forms an algorithm for finding the parametric equations of the envelope. That is, we simply solve equations (A1) and (A6) for x and y in terms of t. See Reference [3] for additional details.

Appendix A2. Developable Surfaces

In general, a surface has a different tangent plane at each point. Hence, the surface may be regarded as the envelope of a two-parameter family of planes. A surface which, has only a one-parameter family of tangent planes is known as a "developable" surface.

Let the equation of the family be

$$F(x_1, x_2, x_3) = 0 \tag{A7}$$

where t is the parameter.

Let S be a surface of the family and let it be intersected by a neighboring surface. If S and S' correspond to the values t and $t + \Delta t$ of the parameter, the intersection curve is represented by the simultaneous equations

$$F(x_1, x_2, x_3, t) = 0 \tag{A8}$$

and

$$F(x_1, x_2, x_3, t + \Delta t) = 0$$

It may also be represented by the equations

$$F(x_1, x_2, x_3, t) = 0$$

$$\frac{F(x_1, x_2, x_3, t + \Delta t) - F(x_1, x_2, x_3, t)}{\Delta t} \tag{A9}$$

The surface $(F(x_1, x_2, x_3, t + \Delta t) - F(x_1, x_2, x_3, t))/\Delta t = 0$ goes through the curve common to the two surfaces $F(x_1, x_2, x_3, t) = 0$ and $F(x_1, x_2, x_3, t + \Delta t) = 0$. When S' approaches S as a limit (that is, when Δt

approaches zero) the intersection curve will, approach a limits curve C. This curve has the representations given by:

$$F(x_1, x_2, x_3, t) = 0$$

$$F_1(x_1, x_2, x_3, t) = 0 \qquad \text{(A10)}$$

When the parameter t varies, the curve C will vary and generate a surface. This surface is the "envelope" of the given family.

Equation (A10), when t is fixed, represents a curve on the surface of the family. The same equations, with t variable, represent the envelope. The result of eliminating t from them is the equation of the envelope. See Reference [3] for additional details.

References

1. Chang, S. H., Huston, R. L., Coy, J. J., "A Computer Aided Design Procedure for Generating Gear Teeth," ASME, Paper No.84-EET-184. Oct. 1984.

2. Buckingham, E. "Involute Spur Gears," Niles-Bement-Pont Co., New York, 1922.

3. Graustein, W. C., Differential Geometry, McMillan, New York, 1935, p. 64.

4. DoCarmo, M. P., Differential Geometry, McMillan, Nw York, 1935, p. 64.

5. Kane, T. R., Analytical Elements of Mechanics, Vol. 2, Academic Press, New York, 1961, 29-47.

6. Lent, D., Analysis and Design of Mechanisms, Prentice Hall, Englewood Cliffs, N. J., 1970, p. 197.

7. Buckingham, E., "Analytical Mechanics of Gears," McGraw Hill, New York, 1949, p. 6.

8. Bonsignore, A. T., "The Effect of Cutter Diameter on Spiral Bevel Tooth Proportions," AGMA 124.20, Oct. 1976.

9. "AGMA Standard Gear Nomenclature - Terms, Definitions, Symbols, and Abbreviations," AGMA Publication 112.05, 1976.

10. "AGMA Reference Information-Basic Gear Geometry," AGMA Publication 115.01, 1959.

11. "AGMA Standard System for Spiral Bevel Gears," AGMA Publication 209.03, 1964.

12. Dyson, A., "A General Theory of the Kinematics and Geometry of Gears in Three Dimensions," Clarendon Press, Oxford, 1969.

13. Coy, J. J., "Geared Power Transmission Technology," NASA Conference Publication 2210, Proceedings of a Symposium held at NASA Lewis Research Center, Cleveland, OH, June 1981, pp. 49-77.

14. Krenzer, T. J., "The Effect of Cutter Radius on Spiral Bevel and Hypoid Tooth Proportions," AGMA 124.20, Oct. 1976.

15. Litvin, F., Petrov, K. and Ganshin, V., "The Effects of Geometric Parameters of Hypoid and Spiroid Gears on their Quality Characteristics," ASME, Journal of Engineering for Industry, Feb. 1974, pp. 330-334.

16. Litvin, F., Krylov, K. and Erichov, M., "Generation of Tooth Surfaces by Two-parameter Enveloping," Mechanism and Machine Theory, Vol. 10, 1975, Pergamon Press, pp. 365-373.

17. Litvin, F., Goldrich, R. N., Coy, J. J., and Zaretsky, E. V., "Precision of Spiral Bevel Gears," ASME Journal of Mechanisms, Transmission, and Automation in Design, Vol. 105, Sept. 1983, pp. 310-316.

18. Litvin, F., Goldrich, R. N., Coy, J. J., and Zretsky, E. V., "Kinematics Precision of Gear Trains," ASME Journal of Mechanisms, Transmission, and Automation in Design, Vol. 105, Sept. 1983, pp. 317-326.

19. Litvin, F., Goldrich, R. N., Coy, J. J., "Precision of Spiral Bevel Gears," ASME, NASA AVRADCOM Technical Report 82-C, 1982.

20. Litvin, F. and Gutman, Ye., "Methods of Synthesis and Analysis for Hypoid Gear Drives of 'Formate' and Helixform,'" P.1, P.2, P.3., ASME, Journal of Mechanical Design, Vol. 103, Jan. 1981, pp. 83-102.

21. Litvin, F. and Gutman, Ye., "A Method of Local Synthesis of Gears Grounded on the Connections Between the Principal and Geodesic Curvatures of Surfaces," ASME Journal of Mechanical Design, Vol. 103, Jan. 1981, pp. 102-113.

22. Litvin, F., Rahman, P., and Goldrich, R. N., "Mathematical Methods for the Synthesis and Optimization of Spiral Bevel Gear Tooth Surfaces," NASA Contractor Report 3553, June 1982.

23. Baxter, M., "Exact Determination of Tooth Surfaces for Spiral Bevel and Hypoid Gears," AGMA Paper #139.02, Oct. 1966.

24. Baxter, M., "Second-Order Surface Generation," Industry Mathematics, Vol. 23, Part 2, 1973, pp. 85-106.

25. Baxter, M. "Effect of Misalignment of Tooth Action of Bevel and Hypoid Gears," ASME Paper #61-MD-20.

26. Baxter, M. L., "Lattice Contact in Generated Spiral Bevel Gears," Journal of Mechanical Design, Vol. 100, Jan. 1978, pp. 41-45.

27. Huston, R. L., and Coy, J. J., "Ideal Spiral Bevel Gears--A New Approach to Surface Geometry," ASME, Journal of Mechanical Design, Vol. 103, Jan. 1981, pp. 127-133.

28. Huston, R. L., and Coy, J. J., "Tooth Profile Analysis of Circular Cut, Spiral Bevel Gears," ASME, Paper 82-DET-79, 1982.

29. Huston, R. L., and Coy, J. J., "Surface Geometry of Circular Cut Spiral Bevel Gears," ASME, Journal of Mechanical Design, Vol. 104, Oct. 1982, pp. 743-748.

30. Huston, R. L., and Coy, J. J., "A Basis for the Analysis of Surface Geometry of Spiral Bevel Gears," NASA Conference Publication 2210, Proceedings of a Symposium held at NASA Lewis Research Center, Cleveland, OH, June 1981, pp. 49-77, 1981.

31. Suzuki, T., Konodo, S., and Ueno, T., "Analysis of Cutting Conditions of Spiral Bevel Gears," Bulletin of JSME, Vol. 24, No. 194, Aug. 1981, pp. 1492-1499.

32. Schultes, T., Raghupathi, P. S., Badawy, A., Altan, T., Wassel, T., and Chevalier, J., "Computer Aided Design and Manufacturing Techniques for Optimum Perform and Finish Forging of Spiral Bevel Gears," TACOM Report #12586, Aug. 1981.

33. Sabroff, A. M., Douglas, J. R., Badawy, A., and Alltan, T., "Application of CAD/CAM Techniques to Close Tolerance Forging of Spiral Bevel Gers," Annual of CIRP, Vol. 31/1, 1981.

34. Fort, P., "Computer Aided Manufacturing and Inspection System for Spiral Bevel Gears," ASME, Paper 80-C2/Det-12, 1980.

35. Uegami, K., and Tamamura, K., "Method of Determining the Actual Form of the Tool Edge from Chips," Bulletin of JSME, Vol. 26, No. 214, Apr. 1983, pp. 641-649.

36. Cloutier, L., and Gosselin, C., "Kinematic Analysis of Bevel Gears," ASME, Paper 84-DET-177, 1984.

37. Winter, H., and Paul. M., "Influence of Relative Displacements Between Pinion and Gear on Tooth Root Stresses of Spiral Bevel Gears," ASME, Journal of Mechanisms, Transmission, and Automation in Design, Vol. 107, Mar 1985, pp. 43-48.

38. Dudley, W. D., "Gear Handbook," McGraw Hill, New York, 1962. Chapter 12.

39. Drozda, T. J., and Wick, C., Ed., "Tool and Manufacturing Engineers Handbook," 14th Edition, Society of Manufacturing Engineers, 1983, Chapter 13.

1. Report No.	2. Government Accession No.	3. Recipient's Catalog No.
NASA CR-179611 AVSCOM TR-87-C-13		

4. Title and Subtitle	5. Report Date
Computer Aided Design and Analysis of Gear Tooth Geometry	May 1987
	6. Performing Organization Code

7. Author(s)	8. Performing Organization Report No.
S.H. Chang and R.L. Huston	None
	10. Work Unit No. 1L161102AH45 505-63-51

9. Performing Organization Name and Address	11. Contract or Grant No.
University of Cincinnati Dept. of Mechanical and Industrial Engineering Cincinnati, Ohio 45221-0072	NSG-3188
	13. Type of Report and Period Covered Contractor Report Final

12. Sponsoring Agency Name and Address	14. Sponsoring Agency Code
U.S. Army Aviation Research and Technology Activity - AVSCOM, Propulsion Directorate, Lewis Research Center, Cleveland, Ohio 44135 and NASA Lewis Research Center, Cleveland, Ohio 44135	

15. Supplementary Notes

Project Managers: Fred B. Oswald, Propulsion Systems Division, NASA Lewis Research Center; John J. Coy, Propulsion Directorate, U.S. Army Aviation Research and Technology Activity - AVSCOM, Lewis Research Center, Cleveland, Ohio 44135. S.H. Chang, currently at Watson IBM Research Center, Yorktown Heights, New York; R.L. Huston, Professor of Mechanics and Director of Institute for Applied Interdisciplinary Research.

16. Abstract

A simulation method for gear hobbing and shaping of straight and spiral bevel gears is presented. The method is based upon an enveloping theory for gear tooth profile generation. The procedure is applicable in the computer aided design of standard and nonstandard tooth forms. An "inverse" procedure for finding a conjugate gear tooth profile is presented for arbitrary cutter geometry. The kinematic relations for the tooth surfaces of straight and spiral bevel gears are proposed. The tooth surface equations for these gears are formulated in a manner suitable for their automated numerical development and solution.

17. Key Words (Suggested by Author(s))	18. Distribution Statement
Gears; Spiral bevel gears; Tooth profile; Computer aided design	Unclassified - unlimited STAR Category 37

19. Security Classif. (of this report)	20. Security Classif. (of this page)	21. No. of pages	22. Price*
Unclassified	Unclassified	83	A05

*For sale by the National Technical Information Service, Springfield, Virginia 22161